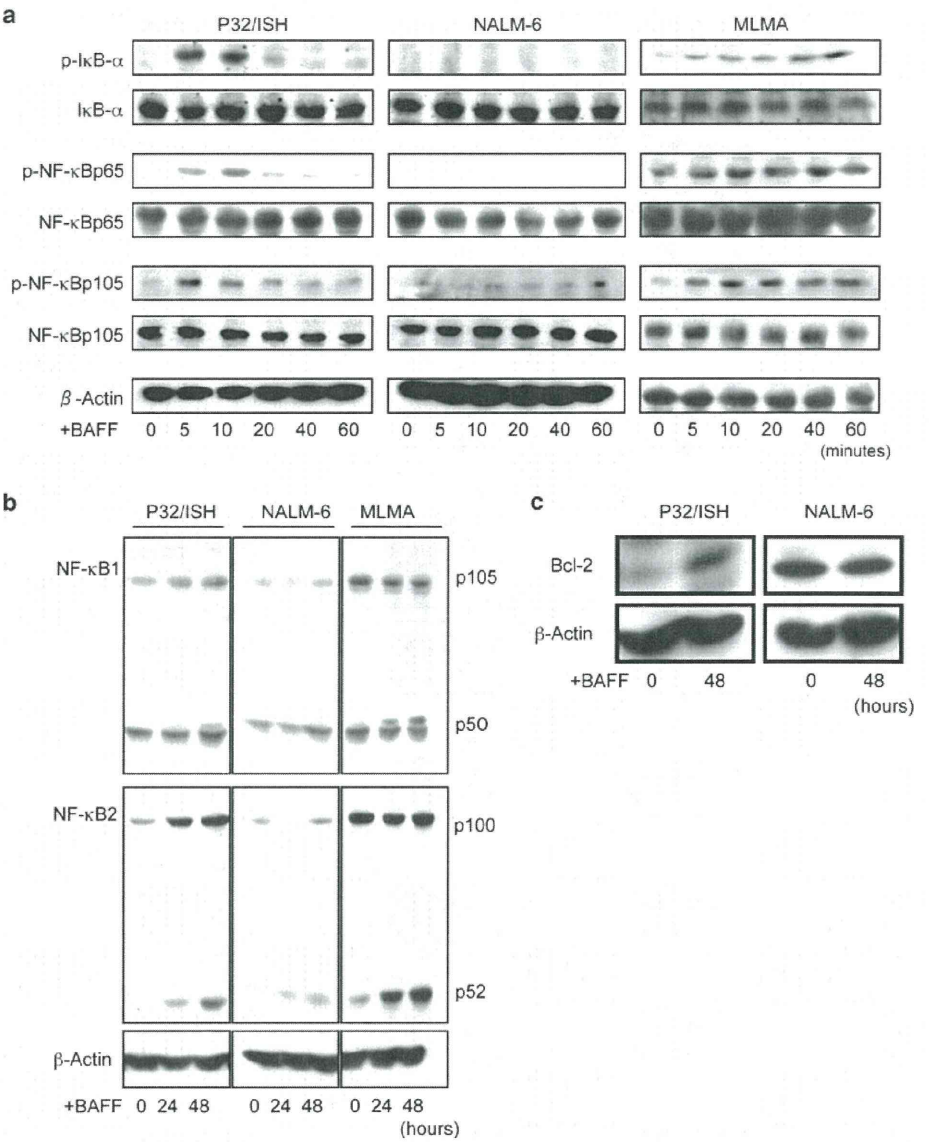

Fig. 6 Comparison between the BAFF-mediated signaling in Burkitt lymphoma (BL) cells and B cell precursor acute lymphoblastic leukemia (BCP-ALL) cells. **a** P32/ISH, NALM-6, and MLMA cells were treated with 200 ng/ml of BAFF, and cell lysates were prepared at the times indicated. Immunoblotting with phospho-specific Abs was performed to detect changes in the phosphorylation state of the proteins indicated. Whole molecules of each protein were included as internal controls. The β-actin protein was also included as internal control. **b** P32/ISH, NALM-6, and MLMA cells were treated with BAFF as in **a**, and cell lysates were prepared at the times indicated. Immunoblotting with Abs specific for either NF-κB1 (precursor form p105, activated form p50) or NF-κB2 (precursor form p100, activated form p52) was performed. The β-actin protein was also detected as internal control. **c** Cell lysates of P32/ISH and NALM-6 cells were examined for Bcl-2 expression as in **b**. The above experiments were repeated three times independently and similar results were obtained

cells. The precise mechanism responsible for the differential effect of BAFF on BL and BCP-ALL cells is unknown. As reported above, major signaling molecules located downstream of BAFF-R were detected in both BL and BCP-ALL cells. However, whereas clear activation of the NF-κB cascade was observed in P32/ISH BL cells, only limited activation was observed in NALM-6 BCP-ALL cells. Up-regulation of CD40 expression following BAFF stimulation was observed in P32/ISH cells, but not in NALM-6 cells. In our preliminary experiments, microarray analysis further suggested that BAFF mediates gene expression in BCP-ALL cells, which is distinct from the gene expression that it mediates in BL cells. Since BCP cells are reported to have a related but different signaling system from mature B cells, it can be speculated that the BCP cells transduce the BAFF-mediated stimuli in a manner that differs from mature B cells and that BAFF-mediated signaling does not mediate the expression of anti-apoptotic molecules in BCP-ALL cells. Further studies of the genes selected above will help to elucidate how BAFF affects BCP-ALL cells and how it is involved in the inhibition of apoptosis in BL cells.

In conclusion, we observed BAFF-R expression in both BL and BCP-ALL cells, which are derived from B cells at different stages of development, and found that BAFF affects tumor cells of these two B-lineage malignancies in a different manner. Since BAFF seems to be involved in survival and/or proliferation of tumor cells of these two B-lineage malignancies, it might be possible to develop a novel approach for the treatment of BL and BCP-ALL by

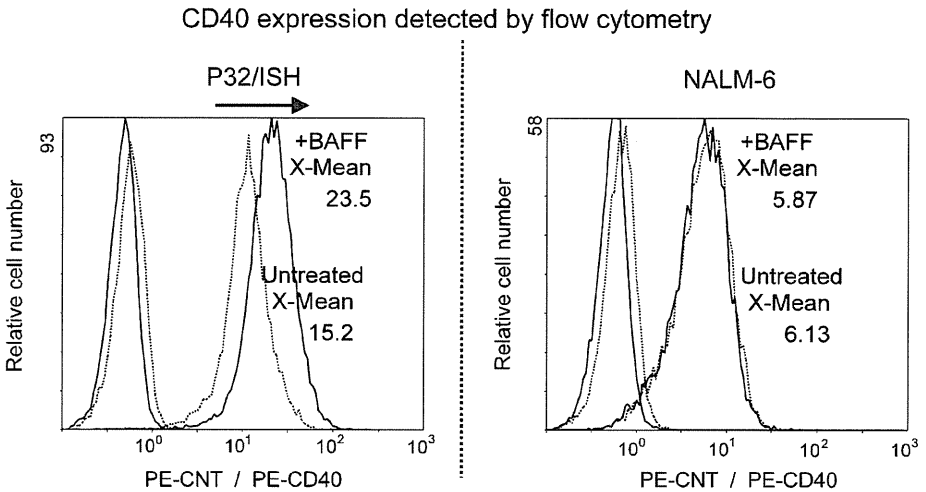

Fig. 7 Effect of BAFF on CD40 expression in P32/ISH and NALM-6 cells. Cells were cultured for 24 h with (+BAFF, *dark lines*) or without (untreated, *light lines*) BAFF 200 ng/ml and examined for the level of CD40 expression by flow cytometry. The histograms of the negative controls are superimposed and shown in each panel (on the *left side*)

targeting BAFF signaling. Although more detailed experiments are clearly needed, our findings in this study should provide a model for investigating the molecular basis of the developmental stage-dependent effect of BAFF on B cells in vitro and help elucidate how BAFF affects early B cell development.

Acknowledgments We thank Dr. K. J. Mori and Dr. Y. Matsuo for the gift of murine BM stromal cell line MS-5 and BL/BCP-ALL cell lines, respectively. We also thank Ms. H. Kiyokawa for her assistance in preparing the manuscript. This work was supported by a grant from the Japan Health Sciences Foundation for Research on Publicly Essential Drugs and Medical Devices (KHA1004), Health and Labour Sciences Research Grants (the 3rd-term comprehensive 10-year-strategy for cancer control H19-010), and a Grant for Child Health and Development from the Ministry of Health, Labour and Welfare of Japan.

Conflict of interest statement We have no financial relationships or conflicts of interest related to this manuscript.

References

1. Mackay F, Silveira PA, Brink R. B cells and the BAFF/APRIL axis: fast-forward on autoimmunity and signaling. Curr Opin Immunol. 2007;19:327–36.
2. Schneider P, MacKay F, Steiner V, et al. BAFF, a novel ligand of the tumor necrosis factor family, stimulates B cell growth. J Exp Med. 1999;189:1747–56.
3. Shu HB, Hu WH, Johnson H. TALL-1 is a novel member of the TNF family that is down-regulated by mitogens. J Leukoc Biol. 1999;65:680–3.
4. Mukhopadhyay A, Ni J, Zhai Y, Yu GL, Aggarwal BB. Identification and characterization of a novel cytokine, THANK, a TNF homologue that activates apoptosis, nuclear factor-κB, and c-Jun NH2-terminal kinase. J Biol Chem. 1999;274:15978–81.
5. Moore PA, Belvedere O, Orr A, et al. BLyS: member of the tumor necrosis factor family and B lymphocyte stimulator. Science. 1999;285:260–3.
6. Gross JA, Johnston J, Mudri S, et al. TACI and BCMA are receptors for a TNF homologue implicated in B-cell autoimmune disease. Nature. 2000;404:995–9.
7. Mackay F, Woodcock SA, Lawton P, et al. Mice transgenic for BAFF develop lymphocytic disorders along with autoimmune manifestations. J Exp Med. 1999;190:1697–710.
8. Khare SD, Sarosi I, Xia XZ, et al. Severe B cell hyperplasia and autoimmune disease in TALL-1 transgenic mice. Proc Natl Acad Sci USA. 2000;97:3370–5.
9. Schiemann B, Gommerman JL, Vora K, et al. An essential role for BAFF in the normal development of B cells through a BCMA-independent pathway. Science. 2001;293:2111–4.
10. Gross JA, Dillon SR, Mudri S, et al. TACI-Ig neutralizes molecules critical for B cell development and autoimmune disease. Impaired B cell maturation in mice lacking BLyS. Immunity. 2001;15:289–302.
11. Vora KA, Wang LC, Rao SP, et al. Cutting edge: germinal centers formed in the absence of B cell-activating factor belonging to the TNF family exhibit impaired maturation and function. J Immunol. 2003;171:547–51.
12. Schneider P. The role of APRIL and BAFF in lymphocyte activation. Curr Opin Immunol. 2005;17:282–9.
13. Thompson JS, Schneider P, Kalled SL, et al. BAFF binds to the tumor necrosis factor receptor-like molecule B cell maturation antigen and is important for maintaining the peripheral B cell population. J Exp Med. 2000;192:129–35.
14. Xia XZ, Treanor J, Senaldi G, et al. TACI is a TRAF-interacting receptor for TALL-1, a tumor necrosis factor family member involved in B cell regulation. J Exp Med. 2000;192:137–43.
15. Marsters SA, Yan M, Pitti RM, Haas PE, Dixit VM, Ashkenazi A. Interaction of the TNF homologues BLyS and APRIL with the TNFreceptor homologues BCMA and TACI. Curr Biol. 2000;10:785–8.
16. Shu HB, Johnson H. B cell maturation protein is a receptor for the tumor necrosis factor family member TALL-1. Proc Natl Acad Sci USA. 2000;97:9156–61.
17. Wu Y, Bressette D, Carrell JA, et al. Tumor necrosis factor (TNF) receptor superfamily member TACI is a high affinity receptor for TNF family members APRIL and BLyS. J Biol Chem. 2000;275:35478–85.
18. Thompson JS, Bixler SA, Qian F, et al. BAFF-R, a newly identified TNF receptor that specifically interacts with BAFF. Science. 2001;293:2108–11.

19. Gras MP, Laabi Y, Linares-Cruz G, et al. BCMAp: an integral membrane protein in the Golgi apparatus of human mature B lymphocytes. Int Immunol. 1995;7:1093–106.
20. Kayagaki N, Yan M, Seshasayee D, et al. BAFF/BLyS receptor 3 binds the B cell survival factor BAFF ligand through a discrete surface loop and promotes processing of NF-kB2. Immunity. 2002;10:515–24.
21. Haiat S, Billard C, Quiney C, Ajchenbaum-Cymbalista F, Kolb JP. Role of BAFF and APRIL in human B-cell chronic lymphocytic leukaemia. Immunology. 2006;118:281–92.
22. Novak AJ, Darce JR, Arendt BK, et al. Expression of BCMA, TACI, and BAFF-R in multiple myeloma: a mechanism for growth and survival. Blood. 2004;103:689–94.
23. Moreaux J, Legouffe E, Jourdan E, et al. BAFF and APRIL protect myeloma cells from apoptosis induced by interleukin 6 deprivation and dexamethasone. Blood. 2004;103:3148–57.
24. Chiu A, Xu W, He B, Dillon SR, et al. Hodgkin lymphoma cells express TACI and BCMA receptors and generate survival and proliferation signals in response to BAFF and APRIL. Blood. 2007;109:729–39.
25. Novak AJ, Grote DM, Stenson M, et al. Expression of BLyS and its receptors in B-cell non-Hodgkin lymphoma: correlation with disease activity and patient outcome. Blood. 2004;104:2247–53.
26. Rodig SJ, Shahsafaei A, Li B, Mackay CR, Dorfman DM. BAFF-R, the major B cell-activating factor receptor, is expressed on most mature B cells and B-cell lymphoproliferative disorders. Hum Pathol. 2005;36:1113–9.
27. Wada K, Maeda K, Tajima K, Kato T, Kobata T, Yamakawa M. Expression of BAFF-R and TACI in reactive lymphoid tissues and B-cell lymphomas. Histopathology. 2009;54:221–32.
28. Smith SH, Cancro MP. Cutting edge: B cell receptor signals regulate BLyS receptor levels in mature B cells and their immediate progenitors. J Immunol. 2003;170:5820–3.
29. Suzuki T, Kiyokawa N, Taguchi T, Sekino T, Katagiri YU, Fujimoto J. CD24 induces apoptosis in human B cells via the glycolipid-enriched membrane domains/rafts-mediated signaling system. J Immunol. 2001;166:5567–77.
30. Taguchi T, Takenouchi H, Matsui J, et al. Involvement of insulin-like growth factor-I and insulin-like growth factor binding proteins in pro-B-cell development. Exp Hematol. 2006;34:508–18.
31. Kiyokawa N, Kokai Y, Ishimoto K, Fujita H, Fujimoto J, Hata JI. Characterization of the common acute lymphoblastic leukaemia antigen (CD10) as an activation molecule on mature human B cells. Clin Exp Immunol. 1990;79:322–7.
32. Saito M, Kiyokawa N, Taguchi T, et al. Granulocyte colony-stimulating factor directly affects human monocytes and modulates cytokine secretion. Exp Hematol. 2002;30:1115–23.
33. Kiyokawa N, Lee EK, Karunagaran D, Lin SY, Hung MC. Mitosis-specific negative regulation of epidermal growth factor receptor, triggered by a decrease in ligand binding and dimerization, can be overcome by overexpression of receptor. J Biol Chem. 1997;272:18656–65.
34. Chaouchi N, Vazquez A, Galanaud P, Leprince C. B cell antigen receptor-mediated apoptosis. Importance of accessory molecules CD19 and CD22, and of surface IgM crosslinking. J Immunol. 1995;154:3096–104.
35. Shan D, Ledbetter JA, Press OW. Apoptosis of malignant human B cells by ligation of CD20 with monoclonal antibodies. Blood. 1998;91:1644–52.
36. Mimori K, Kiyokawa N, Taguchi T, et al. Costimulatory signals distinctively affect CD20- and B-cell-antigen-receptor-mediated apoptosis in Burkitt's lymphoma/leukemia cells. Leukemia. 2003;17:1164–74.
37. He B, Chadburn A, Jou E, Schattner EJ, Knowles DM, Cerutti A. Lymphoma B cells evade apoptosis through the TNF family members BAFF/BLyS and APRIL. J Immunol. 2004;172:3268–79.
38. Ogden CA, Pound JD, Batth BK, et al. Enhanced apoptotic cell clearance capacity and B cell survival factor production by IL-10-activated macrophages: implications for Burkitt's lymphoma. J Immunol. 2005;174:3015–23.
39. Taguchi T, Kiyokawa N, Mimori K, et al. Pre-B cell antigen receptor-mediated signal inhibits CD24-induced apoptosis in human pre-B cells. J Immunol. 2003;170:252–60.
40. Saito Y, Miyagawa Y, Onda K, et al. B-cell-activating factor inhibits CD20-mediated and B-cell receptor-mediated apoptosis in human B cells. Immunology. 2008;125:570–90.
41. Kim SJ, Lee SJ, Choi IY, et al. Serum BAFF predicts prognosis better than APRIL in diffuse large B-cell lymphoma patients treated with rituximab plus CHOP chemotherapy. Eur J Haematol. 2008;81:177–84.

Neuroblastoma cells can be classified according to glycosphingolipid expression profiles identified by liquid chromatography-tandem mass spectrometry

TOMONORI KANEKO[1,2], HAJIME OKITA[1], HIDEKI NAKAJIMA[1], KAZUTOSHI IIJIMA[1], NAO OGASAWARA[1,2], YOSHITAKA MIYAGAWA[1], YOHKO U. KATAGIRI[1], ATSUKO NAKAGAWA[3], NOBUTAKA KIYOKAWA[1], TOSHINORI SATO[2] and JUNICHIRO FUJIMOTO[4]

[1]Department of Pediatric Hematology and Oncology Research, National Research Institute for Child Health and Development, Setagaya-ku, Tokyo 157-8535; [2]Department of Biosciences and Informatics, Keio University, Yokohama 223-8522; [3]Division of Diagnostic Pathology, National Medical Center for Children and Mothers; [4]Clinical Research Center, National Center for Child Health and Development, Setagaya-ku, Tokyo 157-8535, Japan

DOI: 10.3892/ijo_xxxxxxxx

Abstract. It is hoped that the gangliosides contained in neuroblastomas (NBs) can be used as outcome predictors. We used liquid chromatography-tandem mass spectrometry (LC-MS) to analyze the gangliosides expressed in 11 NB cell lines. LC-MS analysis detected a number of gangliosides, including acetylated forms, with significantly higher sensitivity than conventional high-performance thin-layer chromatography analysis, and the results revealed that the expression profiles of the gangliosides GD1a, GD2, and acetylated GD2 differed according to the NB cell line. Hierarchical clustering based on the ganglioside expression profiles obtained by LC-MS analysis revealed that the NB cell lines could be classified into three types according to their expression of these three gangliosides: A-type characterized by high expression of GD1a and low or no expression of GD2/acetylated GD2, B-type characterized by low or no expression of GD1a and high expression of GD2/acetylated GD2, and AB-type characterized by expression of both GD1a and GD2/acetylated GD2. Interestingly, all three *MYCN* non-amplified cell lines were classified into the A-type. The classification was found to be correlated with mRNA expression of ganglioside synthase and neural-differentiation-related genes. The results of this study indicate that LC-MS analysis is useful as a tool for glycosphingolipid research on malignancies.

Correspondence to: Dr Nobutaka Kiyokawa, Department of Pediatric Hematology and Oncology Research, National Research Institute for Child Health and Development, 2-10-1, Okura, Setagaya-ku, Tokyo 157-8535, Japan
E-mail: nkiyokawa@nch.go.jp

Abbreviations: BSA, bovine serum albumin; *CHGA, chromogranin A*; EIC, extracted ion chromatogram; ESI, Electrospray ionization; GM2, GalNAcß1-4(NeuAcα2-3)Galb1-4GlcCer; GD1a, NeuAcα2-3Galb1-3GalNAcß1-4(NeuAcα2-3)Galß1-4GlcCer; GD1b, Galß1-3GalNAcß1-4(NeuAcα2-8NeuAcα2-3)Galß1-4GlcCer; GD2, GalNAcß1-4(NeuAcα2-8NeuAcα2-3)Galß1-4GlcCer; GD3, NeuAcα2-8NeuAcα2-3Galß1-4GlcCer; GM1a, Galß1-3(NeuAcα2-6)GalNAcß1-4Galß1-4GlcCer; GM3, NeuAcα2-3Galß1-4GlcCer; GQ1b, NeuAcα2-8NeuAcα2-3Galß1-3GalNAcß1-4(NeuAcα2-8NeuAcα2-3)Galß1-4GlcCer; GT1a, NeuAcα2-8NeuAcα2-3Galß1-3GalNAcß1-4(NeuAcα2-3)Galß1-4GlcCer; GT1b, NeuAcα2-3Galß1-3GalNAcß1-4(NeuAcα2-8NeuAcα2-3)Galß1-4GlcCer; Ac-GD2, acetylated GD2; HPTLC, high-performance thin-layer chromatography; HRP, horseradish peroxidase; IT, ion trap; LC-MS, liquid chromatography in combination with mass-spectrometry; mAb, monoclonal antibody; MS/MS, tandem mass spectrometry; *MYCN, v-myc myelocytomatosis viral related oncogene*; *N-CAD, N-cadherin*; *NCAM, neural cell adhesion molecule*; *NB, neuroblastoma*; *NF-H, neurofilament 200 kDa subunit*; *NF-M, neurofilament 160 kDa subunit*; *PBS, phosphate-buffered saline*; *Phox2a, paired-like (aristaless) homeobox 2a*; *Phox2b, paired-like homeobox 2b*; *PTN, pleiotrophin*; RT-PCR, reverse transcription-PCR; *TrkA, neurotrophic tyrosine kinase, receptor, type 1*; *TrkC, neurotrophic tyrosine kinase, receptor, type 3*

Key words: glycosphingolipid, neuroblastoma, LC-MS

Introduction

Ganglioside molecules consist of a sialic acid-containing hydrophilic oligosaccharide chain and a hydrophobic lipid anchor ceramide, and they are embedded in the outer leaflet of the plasma membrane and involved in various cellular processes (1). As summarized in Fig. 1, ganglioside biosynthesis occurs in a series of stepwise glycosylations via two main pathways. One pathway results in the synthesis of GM2, GM1a, GD1a and GT1a (referred to as pathway a in this report), and the other pathway results in the synthesis of GD3, GD2, GD1b, GT1b and GQ1b (referred to as pathway b in this report). Both pathways proceed from a common precursor, GM3, which is derived from lactosylceramide (2). Analogous steps in biosynthesis pathways a and b are catalyzed by the same glycosyltransferases (Fig. 1) (1). Some

gangliosides are expressed aberrantly in many types of tumors and are related to the malignant behavior of their cells (3). Research on oligosaccharide chains, however, has not progressed very far because of a lack of effective methods of analyzing oligosaccharide chains. For example, high-performance thin-layer chromatography (HPTLC), a commonly used method to analyze the ganglioside composition of cells, requires large samples and has limited sensitivity for ganglioside detection. Recently improved mass-spectrometry technology, however, may provide an ideal method for analysis of oligosaccharide chains.

Neuroblastomas (NBs) are common solid tumors in childhood and frequently occur in sympathetic ganglia and the adrenal medulla, both of which are derived from the neural crest. The clinical behavior of NBs is known to be varied. The NBs with favorable prognosis often differentiate to mature elements of sympathetic ganglia or regress spontaneously, whereas the NBs with unfavorable prognosis are resistant to chemotherapy, and their long-term outcome remains very poor despite the recent advance in the therapy for NBs. The outcome of NB patients is currently predicted on the basis of a set of risk factors, including age at diagnosis, advanced tumor stage, histological classification according to the international neuroblastoma pathology classification, *MYCN* amplification, DNA diploidy and chromosomal loss of 1p in tumors (4). Even when all of these markers are used in combination, it is sometimes difficult to correctly classify the aggressiveness of NBs, and additional markers that can be used as outcome predictors need to be discovered to establish a more effective therapeutic strategy (5).

Previous reports have described a link between expression of certain ganglioside molecules and the behavior of NBs, suggesting that expression of specific gangliosides by NBs may have diagnostic and prognostic potential (6-9). For example, NB cells express a higher level of GD2 than normal brain cells do (10). Characterization of ganglioside expression in the NBs of infants has revealed higher total pathway b ganglioside levels than in older children (8). By contrast, the unfavorable type of NB cells express lower levels of pathway b gangliosides, especially of GD1b, GT1b and GQ1b, than the non-progressive type of NB cells do (9). Based on the above evidence, we are focusing on ganglioside expression as a possible additional marker for predicting the outcome of NB.

In the present study we attempted to determine the overall profile of ganglioside expression in NB cell lines and in greater detail by using liquid chromatography in combination with mass-spectrometry (LC-MS) to determine levels of glycolipid expression. We then classified 11 NB cell lines into three groups based on their ganglioside expression profiles, especially their profiles of GD1a, GD2 and acetylated GD2 expression, and the classification was found to be correlated with the expression of neural-differentiation-related genes.

Materials and methods

Cell culture and antibodies (Abs). Eleven NB cell lines were used in this study. Nine of the cell lines, GOTO, NB1, NB9, NB16, NB69, IMR32, CHP126, CHP134 and KP-N-NS, were obtained from the Riken Cell Bank (Tsukuba, Ibaraki, Japan), and the other two cell lines, SK-N-SH and SK-N-RA, were a kind gift from Dr P. Reynolds. The characteristics of the cell lines are summarized in Table I. The *MYCN* gene is amplified in eight of these cell lines but not in the other three (NB69, SK-N-SH and SK-N-RA). The cells were cultured at 37˚C in RPMI-1640 (Sigma-Aldrich Co, St. Louis, MO) supplemented with 10% FBS (Sigma) under a humidified atmosphere of 5% CO_2.

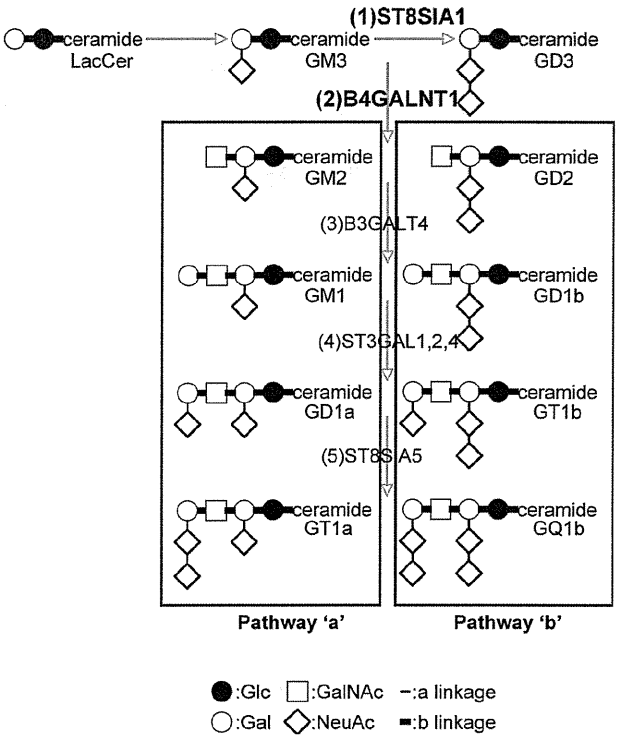

Figure 1. The pathways of ganglioside biosynthesis. The ganglioside biosynthesis pathways and glycosyltransferases that catalyze the synthesis of each ganglioside are shown. The glycosyltransferases whose mRNA expression level was investigated by RT-PCR in this study are indicated in bold type. 1: ST8SIA1, α2,8-sialyltransferase 1 (GD3 synthase); 2: B4GALNT1, ß1,4-N-acetylgalactosaminyltransferase 1 (GM2/GD2 synthase); 3: B3GALT4, ß1,3-galactosyltransferase 4 (GM1/GD1b synthase); 4: ST3GAL1,2,4, α2,3-sialyltansferase 1,2,4 (GD1a/GT1b synthase); 5: ST8SIA5, α2,8-sialyltransferase 5 (GT1a/GQ1b synthase).

Lipid extraction. The lipids were extracted from the cell pellet with 2 ml of chloroform/methanol (2:1, v/v) and then with 2 ml of chloroform/isopropanol/water (7:11:2, v/v) in a sonicated bath. Total extracts were combined and evaporated to dryness. The lipids extracted from the cells were desalted by a SepPak C18 column (Waters, Milford, MA) and analyzed by HPTLC and LC-MS/MS as described below.

HPTLC analysis. TLC chemical staining and immunostaining were performed according to a previously described method (11). Briefly, the lipids were separated on plates

Table I. The summary of characteristics of the cell lines.

Cell line	Origin	Age (months)	Sex	Stage	MYCN[a]	Author/refs.
GOTO	Left adrenal gland	13	Male	IV	Amp	Sekiguchi *et al* ( )
NB1	Neck lymph node	33	Male	IV	Amp	Miyake *et al* ( )
NB9	Adrenal gland	22	Male	IV	Amp	Gilbert *et al* ( )
NB16	Bone marrow	35	Female	IV	Amp	Gilbert *et al* ( )
NB69	Adrenal gland	16	Male	III	Not amp	Gilbert *et al* ( )
IMR32	Abdomen	13	Male	IV	Amp	Tumilowicz *et al* ( )
CHP126	Retroperitoneum	14	Female	III	Amp	Schlesinger *et al* ( )
CHP134	Left adrenal gland	13	Male	IV	Amp	Schlesinger *et al* ( )
KP-N-NS	Brain	10	Female	IV	Amp	Yoshihara *et al* ( )
SK-N-SH	Bone marrow	48	Female	IV	Not amp	June *et al* ( )
SK-N-RA[b]					Not amp	Helson, unpublished

[a]Amplification of MYCN.

precoated with Silica gel 60 (HPTLC sheets, Merck, Darmstadt Germany) by using a solvent system consisting of chloroform/methanol/water containing 0.2% $CaCl_2$ (5:4:1, v/v/v) in duplicate. The HPTLC plates were stained with resorcinol to detect the separated gangliosides. The ganglioside levels were quantitated after scanning the plates on a TLC scanner (model GS-930, Shimadzu). In parallel, other plates were dipped in a 0.1% polyisobutylmethacrylate (Sigma) cyclohexane solution for 1 min and blocked with 1% bovine serum albumin (BSA) in phosphate-buffered saline (PBS). The plates were incubated with the appropriate combination of primary Ab and HRP-conjugated secondary Ab, and then washed thoroughly. The Abs that bound to the plates were visualized with enhanced chemiluminescence reagent SuperSignal (Pierce, Rockford, IL) and detected by LAS-1000 (Fuji Film, Tokyo, Japan).

Acetylated GD2 (Ac-GD2) was detected as described previously (12). After chromatography, the O-acetyl groups were removed from the gangliosides by exposing the TLC plate to concentrated vapor of ammonium hydroxide in a closed chromatography tank for 12 h, and then allowing the plates to dry. The deacetylated chromatogram was immunostained with anti-GD2 Ab as described above.

LC/ESI-MS analysis. The extracted lipids were separated by high-performance LC (1200 series Capillary LC System, Agilent) equipped with a normal-phase column (Imtakt UK-silica, 150 x 0.3 mm). Chloroform/methanol/50 mM acetic acid-triethylamine in water (pH 4.2) = 83/16/1 (A) and methanol/50 mM acetic acid-triethylamine in water (pH 4.2) = 3/1 (B) were used as the solvents to determine the lipid composition. Elution was achieved with a linear gradient of 0-100% of B over 45 min at a flow rate of 3 μl/min. On-line MS and MS/MS were performed by using an Electrospray ionization (ESI)/ion trap (IT) type mass spectrometer (ESI-IT, Bruker Daltonics, Billerica, MA). The lipids were detected by the negative ion mode. The analytical conditions were set to 250°C for capillary temperature and m/z 150-2500 scan range.

Reverse transcription-PCR (RT-PCR) analysis. Total RNA was extracted from cells with an RNeasy Mini Kit (Qiagen, Valencia, CA), and cDNA was generated from 150 ng total RNA by using a FirstStrand cDNA Synthesis Kit (Pharmacia Biotech, Uppsala, Sweden). RT-PCR was performed by using a HotStarTaq Master Mix Kit (Qiagen) according to the manufacturer's protocol. The sets of primers used in this study are listed in Table II. The genes encode enzymes, those involved in gangliosides biosynthesis pathways indicated in Fig. 1, were examined for their expression. The products were separated on a 2% agarose gel and visualized by ethidium bromide staining.

Clustering analysis. The hierarchical clustering heat map was generated by using package R software (http://www.r-project.org/).

Results

Analysis of the composition of the gangliosides in NB cells by LC-MS. We established a condition of glycosphingolipid analysis by LC-MS that enables glycosphingolipid expression by cells to be determined. The lipids extracted from NB cells were separated by HPLC and analyzed by MS connected to HPLC on-line. All glycolipid species, the components considered to have ceramide backbones by LC-MS detection, were subjected to tandem mass spectrometry (MS/MS), and the molecular species was determined.

The extracted ion chromatogram (EIC) and the mass spectrum of the gangliosides extracted from the CHP134 cells are shown in Fig. 2 and Table III as an example of the results of an analysis. The EIC of the gangliosides and the acetylated gangliosides were superimposed in Fig. 2A and B, respectively. The expression levels of the gangliosides were quantified by calculating the areas of each peak on these chromatograms. Fig. 2C shows the MS/MS spectrum of the ion at m/z 1645.8 as a precursor and the structure of the molecular species characterized by the MS/MS fragment ions. The spectrum mainly consists of Y

Table II. The sets of primers used in this study.

Name of gene	Forward primer	Reverse primer
ST8SIA1	TGGGAAATGGTGGGATTCT	TGACAAAGGAGGGAGATTGC
B4GALNT1	GCTGCCTTAGAGCGTTAGACA	GCGAGCAGAAGGACCAGA
B3GALT4	AGGCAGGAACAGGACCTTCT	CCCATATCGCTGTCTTTAGTGAG
ST3GAL1	CAAATCCCGGAAACTCCAG	AGGAAGATGAAATCTGAAAATGGT
ST3GAL2	GTCCAGAGGTGGTGGATGAT	CAGCACCTCATTGGTGTTGT
ST3GAL4	GACCATCCTGAGTGATAAGAAGC	TTAGGATTGACATCCCAGATGA
ß-actin	CACCATGTACCCTGGCATT	GCCGATCCACACGGAGTA
NF-M	CAGGACCTCCTCAACGTCA	CACCCTCCAGGAGTTTTCTG
NF-H	CCGACATTGCCTCCTACC	GGCCATCTCCCACTTGGT
NCAM	AGTTTCTCTGCAGGTGGATATTG	GGCATCTCCTGCCACTTG
CHGA	GCGGTTTTGAAGATGAACTCTC	GCTCTTCCACCGCCTCTT
p75	GGATCTGATGCTCAAGATGGT	GTCTCTCTCTCTTCACTGGATGG
Phox2a	CACTACCCCGACATTTACACG	GCTCCTGTTTGCGGAACTT
Phox2b	CTACCCCGACATCTACACTCG	CCTGCTTGCGAAACTTGG
MYCN	CCACAAGGCCCTCAGTACC	CCTCTTCATCATCTTCATCATCTG
p73	ACGTTTGAGCACCTCTGGA	CGCCCACCACCTCATTATT
TrkA	AGGAAGGCCATTCTCTGCTAC	GGCTGAAGTCTTTGGAGAGC
TrkB	GGGACGTGTACAGCACTGACT	CCTGTACATGATGCTCTCTGGA
TrkC	TCTGGGAGATCTTCACCTATGG	CTTGGGTAATGCACTCAATGAC
N-cadherin	CCTGAAGCCAACCTTAACTGA	TGGAGGGATGACCCAGTCT
PTN	AACTGACCAAGCCCAAACCT	GGTGACATCTTTTAATCCAGCA

Table III. Fragment ions detected by LC-MS/MS spectra of endogenous GSLs from CHP134 cells.

Parent (m/z)	Fragments
GM3 (1152.2, $[M-H]^-$)	1133.6, 860.5, 698.4, 680.4, 536.4, 518.4
GM2 (1355.5, $[M-H]^-$)	1339.4, 1156.6, 1063.6, 860.5, 698.5, 680.4, 536.5
GM1 (1517.2, $[M-H]^-$)	1498.5, 1456.6, 1438.6, 1225.6, 1063.6, 1045.6, 860.6, 698.5, 680.4, 536.5
GD1a (903.9, $[M-2H]^{2-}$)	1516.6, 1498.6, 1225.5, 1151.4, 1063..5, 997.5, 860.5, 680.4, 536.6, 290.0
GT1a (1049.6, $[M-2H]^{2-}$)	1810.4, 1516.5, 1226.4, 903.2, 581.1, 537.2
GD3 (721.4, $[M-2H]^{2-}$)	1151.5, 1133..6, 860.5, 698.5, 581.1, 537.4, 290.0
GD2 (822.9, $[M-2H]^{2-}$)	1354.6, 1337.6, 1063.6, 860.5, 698.5, 680.4, 581.1, 536.4, 290.0
GD1b (904.0, $[M-2H]^{2-}$)	1516.6, 1498.6, 1225.6, 1064.6, 1046.4, 997.5, 860.5, 698.5, 680.4, 581.1, 536.5, 290.0
GT1b (1049.6, $[M-2H]^{2-}$)	1807.5, 1789.4, 1516.7, 1499.6, 1225.5, 1064.666, 903.8, 860.6, 680.4, 581.1, 537.2, 290.1
AcGD1a (925, $[M-2H]^{2-}$)	1558.4, 1516.6, 1225.6, 1151.8, 1064.7, 860.6, 698.4, 680.0, 536.4, 332.2, 290.0
Ac-GD3 (743.0, $[M-2H]^{2-}$)	1151.5, 860.5, 698.4, 680.4, 623.2, 536.5, 332.0, 290.0
Ac-GD2 (843.9, $[M-2H]^{2-}$)	1354.6, 1063.6, 860.5, 698.5, 680.4, 623.1, 536.5, 332.2, 290.0
Ac-GD1b (925.1, $[M-2H]^{2-}$)	1516.5, 1225.6, 1063.5, 1045.6, 860.5, 698.5, 623.1, 536.5, 332.1, 290.0
Ac-GT1b (1070.6, $[M-2H]^{2-}$)	1516.5, 1048.2, 623.6
A (758.4, $[M-2H]^{2-}$)	1225.5, 1063.4, 860.4, 698.4, 536.5, 290.1
B (860.0, $[M-2H]^{2-}$)	1428.5, 1063.6, 1038.2, 997.4, 876.1, 698.6, 673.1, 536.4, 289.9
C (940.8, $[M-2H]^{2-}$)	1590.5, 1429.6, 1411.6, 1225.5, 1063.5, 860.6, 698.6, 536.4, 290.0

ions, i.e., the Y3α at m/z 1354.6 (loss of outer sialic acid), Y2α at m/z 1063.6 (loss of inner sialic acid), Y2α/Y2ß at m/z 860.5 (loss of outer GalNAc), Y1 at m/z 698.5 (Lac-Cer) and Y0 at m/z 536.5 [Cer, the sphingosine (d18:1) with

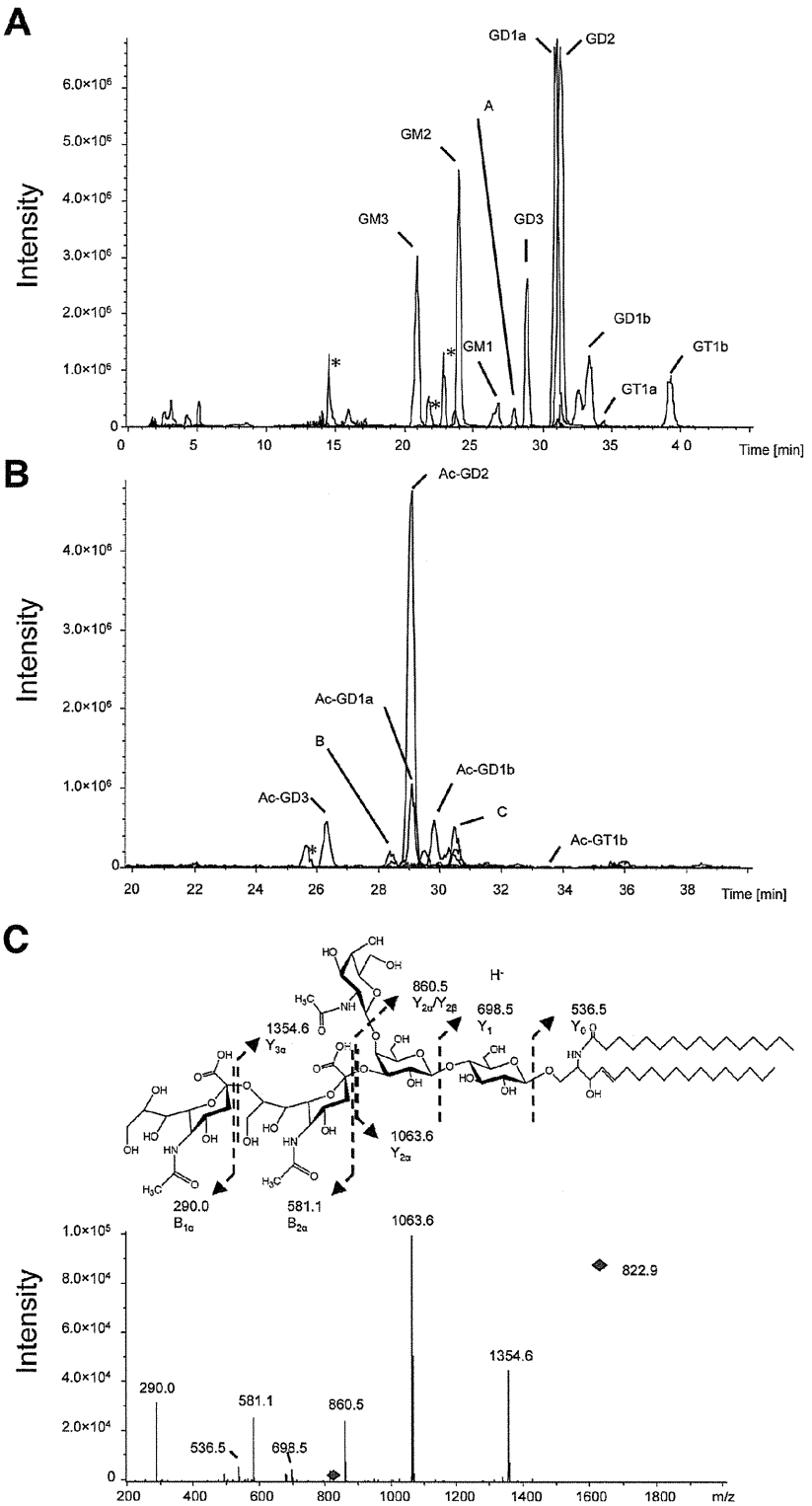

Figure 2. The LC-MS analysis of gangliosides extracted from the CHP134 cells. (A) Superimposed EIC of GM3, GM2, GM1, peak A, GD3, GD1a, GD2, GD1b, GT1a and GT1b extracted from $2x10^6$ of CHP134 cells. (B) Superimposed EIC of Ac-GD3, peak B, Ac-GD1a, Ac-GD2, Ac-GD1b, peak C and Ac-GT1b extracted from $2x10^6$ of CHP134 cells. Asterisks indicate the impurity peak that did not represent molecular species of ceramide. (C) The MS/MS spectrum of the ion at m/z 822.9 $[M-2H]^{2-}$ as a precursor and the chemical structure of the molecular species characterized by the MS/MS fragment ions. All fragment ions appeared as singly charged species.

C16:0 fatty acid] (Fig. 2C). Two B ions, i.e., B1α at m/z 290.0 (Neu5Ac) and B2α at m/z 581.1 (Neu5Ac-Neu5Ac), were also detected (Fig. 2C). Since these fragment patterns corresponded to those of standard GD2 (data not shown), the

Table IV. Ganglioside composition of human neuroblastoma cell lines (Cer: d 18:1/16:0).

	% of total gangliosides										
	SK-N-SH	SK-N-RA	NB69	GOTO	NB9	CHP134	KP-N-NS	IMR32	NB1	NB16	CHP126
GM3	44.44	17.04	11.05	13.02	6.43	7.28	4.00	11.50	13.19	18.11	4.96
GM2	9.93	8.63	22.19	31.77	21.55	11.51	11.34	31.31	23.41	17.75	20.54
GM1	9.72	11.04	12.86	4.43	4.80	8.22	6.56	5.52	4.63	8.30	4.20
GD1a	29.13	33.38	23.30	33.53	53.29	19.31	21.14	7.62	5.20	7.01	8.40
GT1a	0.00	0.00	0.00	0.00	0.00	0.15	0.27	0.00	0.00	0.00	0.00
GD3	0.48	13.23	1.35	2.05	2.71	6.17	3.99	3.67	4.61	4.23	3.75
GD2	0.10	3.97	4.25	7.59	3.77	21.43	23.94	21.88	26.60	25.99	37.11
GD1b	0.47	5.38	7.29	0.00	0.00	6.21	12.89	0.45	0.62	2.25	7.36
GT1b	0.04	1.52	0.10	0.14	0.51	2.94	3.40	0.12	0.09	0.45	0.93
AcGD1a	0.52	0.61	0.56	1.30	1.77	1.46	1.61	0.28	0.28	0.42	0.33
AcGD3	0.00	0.71	0.00	0.07	0.00	1.15	0.00	0.33	1.24	0.26	0.28
AcGD2	0.00	0.77	0.66	1.48	0.65	7.83	7.71	9.17	13.78	12.07	9.17
AcGD1b	0.00	0.00	0.00	0.00	1.02	1.53	1.35	0.41	0.45	0.81	0.83
AcGT1b	0.00	0.00	0.00	0.00	0.00	0.03	0.00	0.00	0.00	0.00	0.00
A	0.00	0.00	5.95	0.99	0.41	3.87	0.51	1.84	2.04	0.00	0.00
B	3.09	0.53	1.93	0.22	0.49	0.00	0.62	0.70	0.34	0.77	1.46
C	2.08	3.18	8.49	3.40	2.60	0.93	0.65	5.20	3.53	1.57	0.69

A, NeuAc-Hex+HexNAc+LacCer; B, NeuAc+HexNAc+(Gal-GlcNAc)+LacCer; C, NeuAc+(Gal-GlcNAc)$_2$+LacCer.

structure of the ion at m/z 822.9 $[M-2H]^{2-}$ was identified as that of GD2.

Fragment ions observed by LC-MS/MS spectra of each peak in Fig. 2A and B and the deduced molecular species were listed in Table III. The sugar composition of peak A, B and C did not correspond to ganglio-series gangliosides, and the structure was predicted as NeuAc-Hex+HexNAc+LacCer, NeuAc+HexNAc+Hex-HexNAc+LacCer and NeuAc+(Hex-HexNAc)$_2$+LacCer, respectively.

The composition of the individual gangliosides in each cell line was expressed as a percentage of its peak area to the total area of all of the ganglioside peaks. Since each ganglioside carried at least two major ceramides, d 18:1/16:0 and d 18:1/24:1, a semi-quantitative value of each ganglioside was calculated for each major ceramide having m/z 535.6 and 646.6, and the values are summarized in Table IV (d 18:1/16:0) and Table V (d 18:1/24:1). It should be noted that several gangliosides also carried a few minor ceramide species (d 18:1/18:0, d 18:1/20:0, d 18:1/22:0) (data not shown).

As shown in Tables IV and V, expression of GD1a, one of the pathway a ganglioside, was high in SK-N-SH, SK-N-RA, NB69, GOTO, NB9, CHP134 and KP-N-NS cells and low in IMR32, NB1, NB16 and CHP126 cells, whereas expression of GD2, a pathway b ganglioside, was high in CHP134, KP-N-NS, IMR32, NB1, NB16 and CHP126 cells and low in SK-N-SH, SK-N-RA, NB69, GOTO and NB9 cells.

Interestingly, the gangliosides containing an O-acetylated sialic acid were detected in all of the NB cell lines (Tables IV and V). Acetylation was observed in GD1a, GD3, GD2, GD1b and GT1b, but the proportion of the acetylated-gangliosides varied from cell line to cell line. Expression of Ac-GD2 was high in CHP134, KP-N-NS, IMR32, NB1, NB16 and CHP126 cells, accounting for >10% of all gangliosides in NB1 and NB16 cells, and low in SK-N-SH, SK-N-RA, NB69, GOTO and NB9 cells (Tables IV and V).

Analysis of ganglioside composition by HPTLC. To confirm the reliability of the profiles of ganglioside expression in NB cells obtained by LC-MS, samples of the same lipid extract preparations were analyzed by HPTLC, and the relative amounts of the individual gangliosides they contained were determined by densitometry (Fig. 3, Table VI). Nine bands stained with resorcinol were tentatively assigned to GM3, GM2, GM1, GD3, GD2, GD1a, GD1b, GT1a and GT1b, respectively, by comparing the Rf values with ganglioside standards. All of them were also detected by LC-MS and the expression profiles of these gangliosides were highly consistent with those detected by LC-MS. However, the other gangliosides, including acetylated forms, that were identified by LC-MS were not detected by HPTLC. For example, HPTLC could not detect GD2 in SK-N-SH, SK-N-RA, NB69, GOTO and NB9, although its expression in the cells was detected by LC-MS.

GD2 and Ac-GD2 ganglioside detected by TLC immunostaining. We performed a TLC immunostaining analysis to confirm the differences in the level of GD2 expression among the NB cell lines. As shown in Fig. 4A, the lipid extracts from SK-N-SH, SK-N-RA, NB69, GOTO and NB9 cells were weakly or hardly stained with anti-GD2 mAb 14.G2a (lanes 1-5), whereas those of CHP-134, KP-N-NS, IMR32,

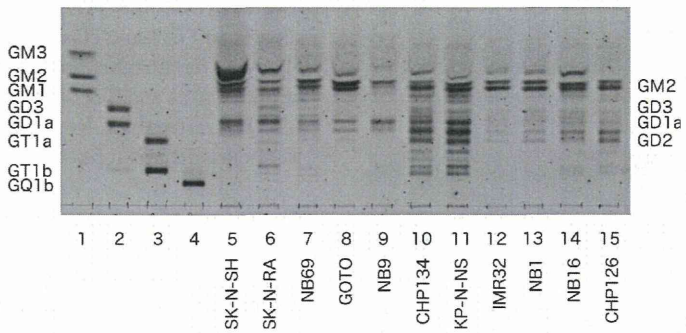

Figure 3. High-performance thin-layer chromatogram of gangliosides extracted from the human neuroblastoma cell lines. Lipids extracted from $1x10^7$ cells were separated on an HPTLC plate and visualized by resorcinol spraying. GM3, GM2, GM1, GD3, GD1a, GT1a, GT1b and GQ1b were used as ganglioside standards (lanes 1-4).

Table V. Ganglioside composition of human neuroblastoma cell lines Cer: d 18:1/24:1.

	% of total gangliosides										
	SK-N-SH	SK-N-RA	NB69	GOTO	NB9	CHP134	KP-N-NS	IMR32	NB1	NB16	CHP126
GM3	36.89	6.22	3.41	4.90	4.80	1.20	0.49	3.05	4.88	7.88	0.60
GM2	8.40	17.05	28.82	15.26	5.93	6.79	8.08	24.80	19.21	12.06	15.25
GM1	7.11	13.94	4.6	7.24	9.65	6.86	5.43	5.19	3.6	6.52	2.44
GD1a	37.09	40.36	45.55	57.80	35.00	29.28	26.75	14.56	8.48	11.58	13.64
GT1a	0.00	0.00	0.00	0.13	0.00	0.25	0.54	0.00	0.00	0.00	0.34
GD3	0.00	1.34	0.79	0.83	20.53	8.10	3.92	3.53	4.89	4.70	2.62
GD2	0.00	2.28	6.70	2.37	3.83	13.05	10.14	25.34	27.55	27.02	40.60
GD1b	1.66	0.00	0.00	0.00	7.11	6.96	19.07	0.89	2.03	3.27	0.00
GT1b	0.00	0.20	0.18	0.87	2.20	3.00	3.35	0.00	0.00	0.61	2.08
AcGD1a	3.04	1.29	3.04	4.56	1.26	2.46	2.61	0.70	0.50	0.74	1.01
AcGD3	0.00	0.00	0.00	0.00	0.00	1.07	0.00	0.31	0.97	0.81	0.00
AcGD2	0.00	0.58	2.64	1.04	1.10	11.07	10.71	14.15	21.59	20.25	16.42
AcGD1b	0.00	0.00	0.00	0.78	3.68	3.19	6.81	0.00	0.92	1.75	2.54
AcGT1b	0.15	0.00	0.00	0.00	0.14	1.68	0.00	0.00	0.00	0.00	0.00
A	0.00	6.19	1.22	0.94	0.00	3.12	0.53	1.64	1.55	0.00	0.00
B	3.97	2.68	0.00	0.79	1.38	0.67	0.82	1.04	0.57	0.77	1.70
C	1.67	7.88	3.04	2.48	3.38	1.26	0.77	4.81	3.27	2.05	0.74

A, [NeuAc-Hex+HexNAc+LacCer; B, [NeuAc+HexNAc+(Gal-GlcNAc)+LacCer; C, [NeuAc+$(Gal-GlcNAc)_2$+LacCer.

Table VI. Ganglioside composition of human neuroblastoma cell lines (HPTLC).

	% of total gangliosides										
	SK-N-SH	SK-N-RA	NB69	GOTO	NB9	CHP134	KP-N-NS	IMR32	NB1	NB16	CHP126
GM3	52.45	20.65	17.56	15.01	7.34	5.92	3.40	11.66	14.09	17.40	7.18
GM2	25.36	29.50	49.09	59.76	42.39	18.83	19.27	63.44	49.54	35.99	34.89
GM1	1.68	1.12	4.84	1.98	0.51	7.81	8.87	2.99	3.80	4.31	5.24
GD1a	20.50	29.27	19.86	20.51	49.75	16.06	13.97		2.17	6.60	0.48
GT1a		2.54	0.28	0.60		6.70	8.85				
GD3		9.26	6.35	2.13		5.86	5.30	10.40	15.08	9.81	11.91
GD2						15.86	15.21	11.52	15.33	21.86	34.22
GD1b						12.18	11.92			0.56	2.04
GT1b		7.66	2.03			10.78	13.22			3.47	4.05

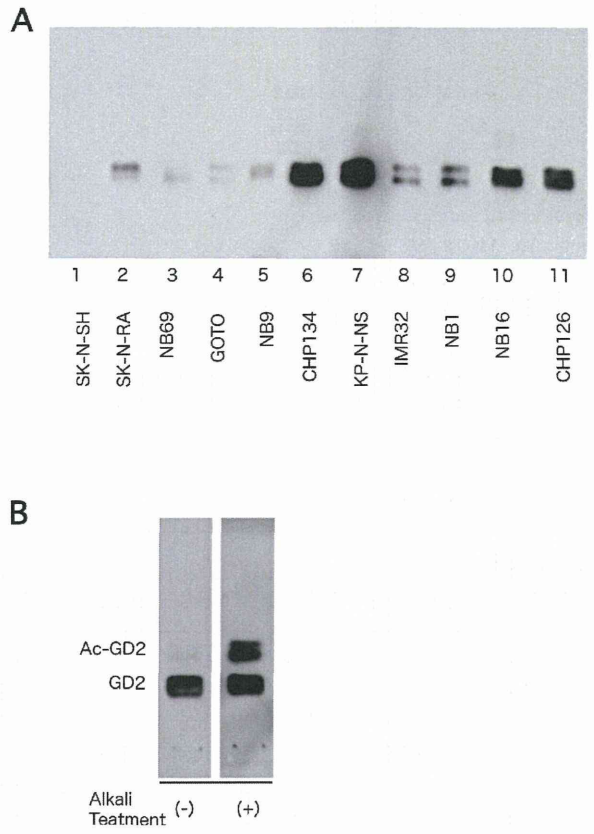

Figure 4. TLC immunostaining of ganglioside GD2 and Ac-GD2. (A) The lipids extracted from $1x10^5$ cells were separated on HPTLC plates and immunostained with mAb 14.G2a. (B) The lipids of $1x10^5$ CHP134 cells separated on an HPTCL plate was treated with alkali and immunostained with mAb.G2a.

NB1, NB16 and CHP126, were strongly or significantly stained (lanes 6-11). These results are essentially consistent with those obtained with LC-MS.

As shown in Fig. 4B, when the TLC plate was treated with alkali after TLC development to remove acetyl group from sialic acid residues, the band newly produced by the conversion of Ac-GD2 to GD2 was detected at a position with a higher Rf value than GD2. Taken together with the results of the LC-MS analysis, these findings show that Ac-GD2 is expressed in NB cells.

Clustering analysis of gangliosides expressed in NB cells. The above results imply that the NB cell lines have distinct glycolipid expression profiles that allow them to be classified in several groups. As shown in Tables IV, V and Fig. 5, the profiles of glycosphingolipid GD1a, GD2 and acetylated GD2 expression varied from cell line to cell line. We therefore performed a clustering analysis centered on these three glycosphingolipids, and the results showed that the NB cell lines could be classified into three groups based on their expression of these three gangliosides (Fig. 5B). The NB9, NB69, SK-N-SH, SK-N-RA and GOTO cells were characterized by high expression of GD1a and low expression of GD2/acetylated GD2 and classified as type A here, whereas CHP126, IMR32, NB1 and NB16 cells were characterized by low expression of GD1a and high expression of GD2/acetylated GD2 and classified as type B. CHP134 and KP-N-NS cells, on the other hand, were characterized by expression of both GD1a and GD2/acetylated GD2 and classified as type AB. Interestingly, all three *MYCN* non-amplified cell lines were classified as type A.

Expression of ganglioside synthase mRNA detected by RT-PCR in NB cell lines. To investigate the relationship between ganglioside expression and the level of expression of enzymes involved in ganglioside biosynthesis, RT-PCR analysis was used to investigate the NB cell lines for mRNA expression of two ganglioside synthases. As shown in Fig. 6A, the results showed a high level of GD3 synthase mRNA expression (ST8SIA1) (Fig. 1) in the types B and AB cell lines, whereas mRNA expression of B4GALNT1, which is responsible for catalyzing the synthesis of both GM2 and GD2 (Fig. 1), was detected in all of the cell lines.

RNA expression of neural differentiation markers detected by RT-PCR in NB cell lines. To investigate the biological significance of the classification of NB cell lines based on their ganglioside expression profile, we investigated expression of neural-differentiation-related genes by RT-PCR and assessed the relation between their expression and glycolipid expression. As shown in Fig. 6B and C, RT-PCR analysis revealed that mRNA expression of the neural-differentiation-related genes *Phox2a* and *b*, *TrkC*, neurofilament, and *N-CAM* was positively correlated with GD2 and acetylated GD2 expression in the NB cell lines. By contrast, mRNA expression of pleiotrophin (*PTN*) tended to be high in cell lines with a low level of GD2 expression. All *MYCN* non-amplified cells show low *MYCN* expression by RT-PCR (Fig. 6D).

Discussion

In this study we used an LC-MS analysis system to detect glycosphingolipid expression in NB cells and clearly demonstrated its great potential as a tool for glycosphingolipid research. As shown above, the LC-MS analysis was highly sensitive and enabled detection of a number of glycolipids expressed in NB cells that were not detected by HPTLC analysis. This approach allows determination of even low percentages of lipids of each molecular species and showed clear differences between the glycosphingolipid profiles of a series of NB cell lines. The method described in this report should be useful and easily adaptable to glycosphingolipid analysis of various types of tumor cells.

In this study we also demonstrated the presence of acetylated forms of gangliosides in NB cells. As described above, we detected acetylated forms of GD1a, GD3, GD2, GD1b and GT1b in NB cells by LC-MS analysis and expression of acetylated GD2 was found to be high. For example, Ac-GD2 accounted for >10% of the total ganglioside in NB1 and NB16 cells. The presence of acetylated GD2 was correlated with expression of GD2. Ye and Cheung demonstrated that O-acetylated GD2 is a naturally occurring ganglioside derivative in human tumors, including in NB, by using mAb 3F8, which specifically recognizes GD213, and our data are consistent with their findings.

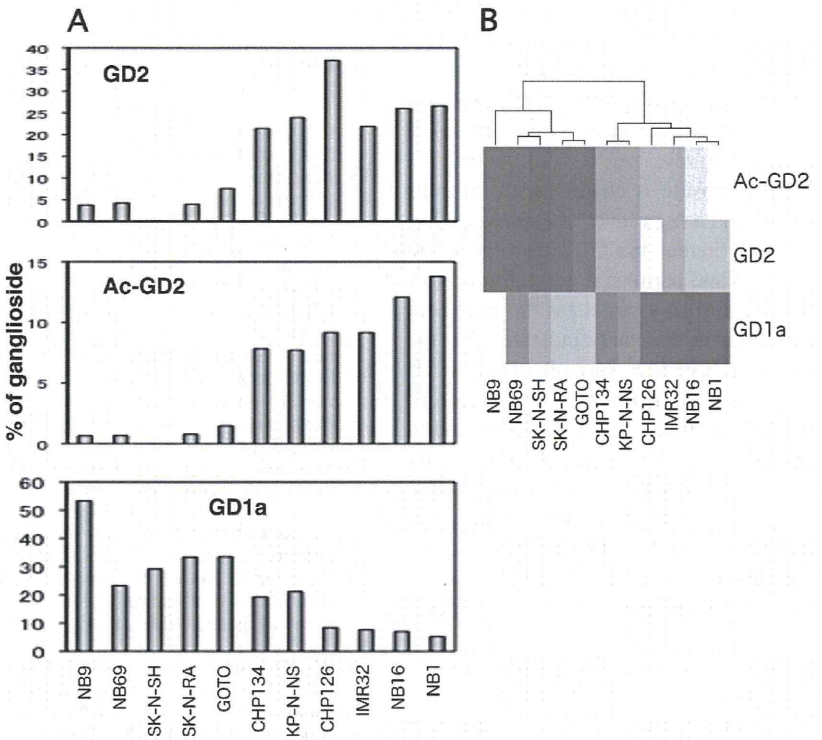

Figure 5. Hierarchical clustering of differentially expressed gangliosides. (A) The percentage of Ac-GD2, GD2 and GD1a to the total gangliosides of NB cell lines. (B) The clustering tree shows the expression pattern and similarity in cell lines. The strength of the gangioside expression was gradually increased on the heat map.

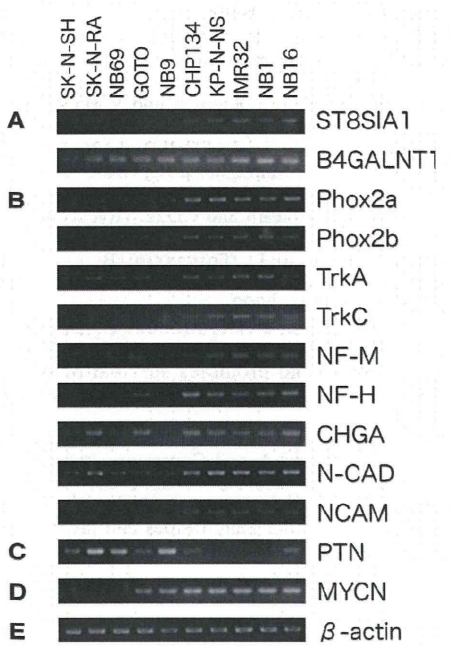

Figure 6. Analysis of expression of neural-differentiation-related genes and glycosyltransferase genes by RT-PCR. (A) Glycosyltransferase genes (Fig. 1), (B) *Phox2a*, paired-like (aristaless) homeobox 2a; *Phox2b*, paired-like homeobox 2b; *TrkA*, neurotrophic tyrosine kinase, receptor, type 1, also known as *NTRK1*; *TrkC*, neurotrophic tyrosine kinase, receptor, type 3, also known as *NTRK3*; *NF-M*, neurofilament 160 kDa subunit; *NF-H*, neurofilament 200 kDa subunit; *CHGA*, chromogranin A; *N-CAD*, N-cadherin and *NCAM*, neural cell adhesion molecule, (C) *PTN*, pleiotrophin, (D) *MYCN*, v-myc myelocytomatosis viral related oncogene, (E) ß-actin was used as an internal control.

The biological significance of ganglioside acetylation has not been fully elucidated, but it is thought to modulate cell function by regulating the ability of gangliosides to bind cell adhesion molecules. For example, CD22ß (also called Siglec-2) is a B-cell-restricted phosphoprotein that mediates interactions with other cells via binding with α2-6-linked sialic acids on glycoconjugates, and the fact that the binding can be inhibited by 9-O-acetylation of sialic acids suggests that CD22ß adhesion events are regulated by ganglioside acetylation (14,15). In childhood acute lymphoblastic leukemia, on the other hand, administration of exogenous GD3 induces apoptosis, whereas O-acetylated GD3 fails to induce similar effects, suggesting that O-acetylation of GD3 promotes leukemia cell survival by preventing apoptosis (16,17). Although the significance of acetylated GD2 in NB cells still remains largely unknown, further investigation should shed light on the functional role of gangliosides in the biological behavior of NB cells.

The NB cell lines were classified into three types based on their of ganglioside expression profiles determined by LC-MS analysis, namely, type A, with a high level of expression of GD1a but low level or no expression of GD2/acetylated GD2, and consisting of SK-N-SH, SK-N-RA, NB69, GOTO and NB9 cells, type B, with a high level of expression of GD2/acetylated GD2 but low level or no expression of GD1a, and consisting of IMR32, NB1, NB16 and CHP126 cells, and type AB, which express both GD1a and GD2/acetylated GD2, and consisting of CHP134 and KP-N-NS cells. The results of the RT-PCR analyses indicated that the ganglioside expression profiles of NBs correlated with their ganglioside

synthase expression pattern. As shown in Fig. 6, ST8sia1, which catalyzes the synthesis of GD3 from GM3, was expressed only in the types B and AB NB cell lines and not in any of the type A NB cell lines, whereas B4galnt1, which catalyzes the synthesis of both GM2 and GD2, was expressed in all the NB cell lines tested in this study.

Expression of GD2 ganglioside is characteristic of cells of neuroectodermal origin, and a high level of expression has been reported in NB cells, whereas the GD2 distribution in humans is limited to neurons and peripheral nerve fibers (18). Thus, GD2 appears to be useful as a target for the treatment of NB. However, our findings in this study indicated that the level of GD2 expression in NB cells is variable and that NB cells can be classified based on their pattern of expression of ganglio-series gangliosides, including GD2. Since increased shedding of GD2 ganglioside and *MYCN* amplification jointly characterize the aggressive type of NB cells (19), classification of NBs based on their ganglioside expression profile may have prognostic value. Our observation that the ganglioside expression profiles are closely related to the expression of neural-differentiation-related genes appears to further support this notion.

In conclusion, we have demonstrated the usefulness of the LC-MS analysis system as a tool for glycosphingolipid research. Eighteen species of glycosphingolipids containing gangliosides of a and b pathways and their acetylated forms were detected. The expression ratios of the glycosphingolipids were determined, and were compared among 11 of NB cell lines. Based on the results, it was indicated that these NB cell lines could be classified into three categories. Although more detailed experiments are clearly needed, further investigations using the new method should provide a new approach to determining the biological significance of glycosphingolipids in NBs and identifying novel biomarkers for predicting the outcome of NB.

Acknowledgments

We are grateful to Dr P. Reynolds for providing the SK-N-SH and SK-N-RA cells. We thank Ms. H. Kiyokawa for her assistance to prepare the manuscript. This work was supported by a grant from the Japan Health Sciences Foundation for Research on Publicly Essential Drugs and Medical Devices (KHA1004), Health and Labour Sciences Research Grants (Research on Human Genome Tailor made and Research on Publicly Essential Drugs and Medical Devices H18-005, the 3rd-term Comprehensive 10-year strategy for Cancer Control H19-010), a Grant for Child Health and Development from the Ministry of Health, Labour and Welfare of Japan, and by CREST, JST. This work was supported in part by the Grant-in-Aid for Cancer Research (16-16) from the Ministry of Health, Labor and Welfare.

References

1. Ledeen RW and Yu RK: Gangliosides: structure, isolation, and analysis. Methods Enzymol 83: 139-191, 1982.
2. Van Echten G and Sandhoff K: Ganglioside metabolism. Enzymology, topology, and regulation. J Biol Chem 268: 5341-5344, 1993.
3. Hakomori S: Tumor malignancy defined by aberrant glycosylation and sphingo(glyco)lipid metabolism. Cancer Res 56: 5309-5318, 1996.
4. Weinstein JL, Katzenstein HM and Cohn SL: Advances in the diagnosis and treatment of neuroblastoma. Oncologist 8: 278-292, 2003.
5. Ohira M, Oba S, Nakamura Y, Hirata T, Ishii S and Nakagawara A: A review of DNA microarray analysis of human neuroblastomas. Cancer Lett 228: 5-11, 2005.
6. Schengrund CL, Repman MA and Shochat SJ: Ganglioside composition of human neuroblastomas. Correlation with prognosis. A Pediatric Oncology Group Study. Cancer 56: 2640-2646, 1985.
7. Schengrund CL and Shochat SJ: Gangliosides in neuroblastomas. Neurochem Pathol 8: 189-202, 1988.
8. Kaucic K, Etue N, LaFleur B, Woods W and Ladisch S: Neuroblastomas of infancy exhibit a characteristic ganglioside pattern. Cancer 91: 785-793, 2001.
9. Hettmer S, Malott C, Woods W, Ladisch S and Kaucic K: Biological stratification of human neuroblastoma by complex B pathway ganglioside expression. Cancer Res 63: 7270-7276, 2003.
10. Wu ZL, Schwartz E, Seeger R and Ladisch S: Expression of GD2 ganglioside by untreated primary human neuroblastomas. Cancer Res 46: 440-443, 1986.
11. Nakamura K, Suzuki M, Taya C, Inagaki F, Yamakawa T and Suzuki A: A sialidase-susceptible ganglioside, IV3 alpha (NeuGc alpha 2-8NeuGc)-Gg4Cer, is a major disialoganglioside in WHT/Ht mouse thymoma and thymocytes. J Biochem 110: 832-841, 1991.
12. Kushi Y, Ogura K, Rokukawa C and Handa S: Blood group A-active glycosphingolipids analysis by the combination of TLC-immunostaining assay and TLC/SIMS mass spectrometry. J Biochem 107: 685-688, 1990.
13. Ye JN and Cheung NK: A novel O-acetylated ganglioside detected by anti-GD2 monoclonal antibodies. Int J Cancer 50: 197-201, 1992.
14. Sjoberg ER, Powell LD, Klein A and Varki A: Natural ligands of the B cell adhesion molecule CD22 beta can be masked by 9-O-acetylation of sialic acids. J Cell Biol 126: 549-562, 1994.
15. Kelm S, Schauer R, Manuguerra JC, Gross HJ and Crocker PR: Modifications of cell surface sialic acids modulate cell adhesion mediated by sialoadhesin and CD22. Glycoconj J 11: 576-585, 1994.
16. Malisan F, Franchi L, Tomassini B, *et al*: Acetylation suppresses the proapoptotic activity of GD3 ganglioside. J Exp Med 196: 1535-1541, 2002.
17. Mukherjee K, Chava AK, Mandal C, Dey SN, Kniep B, Chandra S and Mandal C: O-acetylation of GD3 prevents its apoptotic effect and promotes survival of lymphoblasts in childhood acute lymphoblastic leukaemia. J Cell Biochem 105: 724-734, 2008.
18. Varki A: Glycosylation changes in cancer. In: Essentials of Glycobiology. Varki A and Cummings R (eds). Cold Spring Harbor Laboratory Press, New York, 1999.
19. Valentino L, Moss T, Olson E, Wang HJ, Elashoff R and Ladisch S: Shed tumor gangliosides and progression of human neuroblastoma. Blood 75: 1564-1567, 1990.

Pediatr Blood Cancer 2010;54:212–215

Retrospective Analysis of Non-Anaplastic Peripheral T-Cell Lymphoma in Pediatric Patients in Japan

Ryoji Kobayashi, MD,[1]* Kazumi Yamato, MD,[2] Fumiko Tanaka, MD,[3] Yoshifumi Takashima, MD,[4] Hiroko Inada, MD,[5] Akira Kikuchi, MD,[6] Masa-aki Kumagai, MD,[7] Shosuke Sunami, MD,[8] Atsuko Nakagawa, MD,[9] Reiji Fukano, MD,[10] Naoto Fujita, MD,[11] Tetsuo Mitsui, MD,[12] Masahito Tsurusawa, MD,[13] and Tetsuya Mori, MD,[14] Lymphoma Committee, Japanese Pediatric Leukemia/Lymphoma Study Group

Background. Reports of non-anaplastic peripheral T-cell lymphoma (PTCL) in pediatric patients are relatively rare. ***Procedure.*** We performed a retrospective analysis in patients with PTCL over an 18-year period (1991–2008). ***Results.*** We could analyze clinical data in 21 patients with non-anaplastic PTCL; 10 were female and 10 male. Median age of onset was 11 years (range: 1–21 years). There were nine patients with PTCL, not otherwise specified (PTCL-NOS); ten with extranodal NK/T-cell lymphoma, nasal type; one with angioimmunoblastic T-cell lymphoma; and one with subcutaneous panniculitis-like T-cell lymphoma. Initial lesions involved cervical lymph nodes in five patients, and the skin in five patients. In five patients, hemophagocytic syndrome (HPS) was the initial clinical feature. There were 12 patients with advanced stage disease (stages III and IV). Chemotherapy and radiation was administered in 18 and 2 patients, respectively. Among the two patients who did not receive chemotherapy and radiation, one patient died while being treated for HPS but another improved spontaneously. Although 5 patients relapsed, 18 of 21 patients remained alive without disease at last follow-up. Five-year overall survival rate was 85.2%. ***Conclusions.*** Generally, the outcome results of conventional chemotherapy for high-risk PTCL are poor in adult patients. However, the excellent results in our study suggest that PTCL of childhood is quite different from that of adulthood. Although this study is first report about PTCL of Asian children, the number of patients was small in this study. Larger studies are needed to confirm these findings. Pediatr Blood Cancer 2010;54:212–215. © 2009 Wiley-Liss, Inc.

Key words: child; peripheral T-cell lymphoma

INTRODUCTION

Peripheral T-cell lymphomas (PTCLs) are a heterogeneous group of rare diseases, usually demonstrating clinical aggressiveness [1]. Because of difficulty and variability in diagnosis, improvements in diagnostic technology, and changing classification systems over time, the interpretation of studies is complicated. In addition, the response to current treatments and long-term outcome are generally poor [2–6]. Reports of non-anaplastic PTCL in pediatric patients are relatively rare [7–11]. Moreover, although geographic variation has been well documented, this may reflect exposure to specific pathogenic viruses, such as Epstein Barr (EB) virus and human T-cell leukemia virus-1 in Asian countries. There are no reports about child PTCL from Asia. We therefore performed a retrospective analysis of patients with PTCL over an 18-year period (1991–2008).

METHODS

We performed this retrospective analysis as the lymphoma committee of the Japan Leukemia and Lymphoma Study Group (JPLSG). Data were obtained from the Japan Association of Childhood Leukemia Study (JACLS), Tokyo Children's Cancer Study Group (TCCSG), Japanese Children's Cancer and Leukemia Study Group (JCCLSG), and Kyushu-Yamaguchi Children's Cancer and Leukemia Study Group (KYCCSG). In the 18-year study period, 55 patients were registered as having PTCL or NK/T lymphoma including blastic NK lymphoma and myeloid/NK lymphoma. Clinical data for 21 patients with non-anaplastic PTCL after excluding 34 patients with blastic NK lymphoma and myeloid/NK lymphoma were analyzed.

Pathologic diagnoses were confirmed by central review in 9 of 21 patients. Central review was performed using WHO classification. For the other 12 children, histopathology was performed at the treating center only and confirmed from a copy of the pathology report. In almost all reports, immunophenotyping such as CD79a, CD20, CD3, CD43, TdT, and MPO was included.

DOI 10.1002/pbc.22329
Published online 23 October 2009 in Wiley InterScience (www.interscience.wiley.com)

The presence of an association with EB virus was determined by detection of EB virus genome in white blood cells or plasma, or the detection of this virus in histological material by EB virus encoded small RNA (EBER) in situ hybridization [12].

Statistical Analyses

Analysis of overall survival was performed using the Kaplan–Meier method, with differences compared by log-rank test. Differences between groups were analyzed using a Fisher exact test and a Mann–Whitney *U*-test. Statistical analyses were

[1]Department of Pediatrics, Sapporo Hokuyu Hospital, Shiroishiku, Sapporo, Japan; [2]Department of Pediatrics, Osaka City University School of Medicine, Osaka, Japan; [3]Department of Pediatrics, Saiseikai Yokohamashi Nanbu Hospital, Yokohama, Japan; [4]Department of Hematology and Oncology, Shizuoka Children's Hospital, Shizuoka, Japan; [5]Department of Pediatrics, Kurume University School of Medicine, Kurume, Japan; [6]Department of Pediatrics, Graduate School of Medicine, The University of Tokyo, Tokyo, Japan; [7]Division of Hematology and Oncology, National Center for Child Health and Development, Tokyo, Japan; [8]Department of Pediatrics, Japanese Red Cross Narita Hospital, Narita, Japan; [9]Department of Pathology, National Center for Child Health and Development, Tokyo, Japan; [10]Department of Pediatrics, Yamaguchi University, Yamaguchi, Japan; [11]Department of Pediatrics, Hiroshima Red Cross Hospital and Atomic-bomb Survivors Hospital, Hiroshima, Japan; [12]Department of Pediatrics, Yamagata University, Yamagata, Japan; [13]Department of Pediatrics, Aichi Medical University, Aichi, Japan; [14]Division of Hematology and Oncology, National Center for Child Health and Development, Tokyo, Japan

Grant sponsor: Ministry of Health, Labor and Welfare, Japan.

*Correspondence to: Ryoji Kobayashi, Department of Pediatrics, Sapporo Hokuyu Hospital, Higashi-Sapporo 6-6, Shiroishiku, Sapporo 003-0006, Japan. E-mail: r-koba@jacls.jp

Received 3 July 2009; Accepted 14 September 2009

performed using Dr. SPSS II for Windows (release 11.0.1J, SPSS Japan, Inc.).

RESULTS

In the 18-year study period, we were able to analyze clinical data from 21 patients with non-anaplastic PTCL (Table I). Because 1,711 child and adolescent patients with non-Hodgkin lymphoma were registered in the 18-year period, the proportion of NHL classified as PTCL was 1.2%. Of the 21 patients, 10 were male and 11 were female. Median age of onset was 11 years (range: 1–21 years). There were nine patients with PTCL not otherwise specified (PTCL-NOS); ten with extranodal NK/T-cell lymphoma, nasal type; one with angioimmunoblastic T-cell lymphoma; and one with subcutaneous panniculitis-like T-cell lymphoma. Initial lesions involved the cervical lymph nodes in five patients, and the skin in five patients. In five patients, hemophagocytic syndrome (HPS) was the initial clinical feature. With regard to stage of disease at diagnosis, eight patients were at stages I and II, six were at stage III, and six were at stage IV; this information was not available for one patient. Chemotherapy and radiation were administered in 18 and 2 patients, respectively. Two patients received no treatment. Treatment for PTCL was not consistent in this study. Eight patients received a T-cell lymphoma/leukemia regimen, and four received a B cell lymphoma/leukemia regimen. Among the two patients who did not receive chemotherapy and radiation, one patient died while undergoing treatment for HPS and another improved spontaneously. In the latter patient (patient 5), the initial clinical features were fever, cervical lymphadenopathy, and pancytopenia. He was diagnosed with HPS from laboratory data and bone marrow aspiration. Lymph node biopsy revealed PTCL and there was positive staining on EBER in situ hybridization. However, after several days, the fever abated and laboratory data improved. He received no chemotherapy at the request of his parents and remained disease-free at last follow-up, 9 months after onset.

Eleven patients received stem cell transplantation. Of these, two received an autologous peripheral blood stem cell transplant (PBSCT), five received a related bone marrow transplant (BMT), two received a related PBSCT, two received an unrelated cord blood stem cell transplant (CBSCT), and one received an unrelated BMT. Although 5 patients relapsed, 17 of the 21 patients were alive without disease at last follow-up, giving an overall 5-year survival rate of 85.2% (Fig. 1). Causes of death for the three patients who succumbed to their disease were HPS, progression of disease and complications of stem cell transplantation. Ten of the 21 patients had PTCL associated with EB virus. Compared with patients with extranodal NK/T lymphoma, nasal type, those with PTCL-NOS were younger (median 7 years vs. 15.5 years, $P < 0.05$) and had a lower relapse rate (11% vs. 40%). However, gender (male/female; 5/4 vs. 4/6), proportion with advanced stage disease (56% vs. 60%), survival rate (87.5% vs. 80.0%) and association with EB virus (44% vs. 60%) were similar and statistically non-significant differences.

DISCUSSION

Peripheral NK/T-cell neoplasms are an uncommon group of diseases that show distinct racial and geographic variation. The prognostic significance of the T-cell phenotype has been clearly defined in recent studies by using modern lymphoma classification systems. Anaplastic large cell lymphoma, not rare in childhood, is another type of PTCL. Results of conventional chemotherapy for high-risk PTCL are poor compared with those for their aggressive B-cell counterparts in adult patients.

However, although case reports of pediatric PTCL are sometimes seen [7,10,11], large case series are very rare. The only two such case series published are a report from the United Kingdom [8] and the Children's Oncology Group (COG) Study [9]. In the UK series, 25 cases were identified, 44% of children died and 5-year survival rate was 59%. On the other hand, in the 20 patients in the COG series, 5-year survival rate was 90% in patients with localized disease and 50% in those with advanced disease. In the present study, 21 patients with PTCL were identified; these included 9 with PTCL-NOS; 10 with extranodal NK/T-cell lymphoma, nasal type; 1 with angioimmunoblastic T-cell lymphoma; and 1 with subcutaneous panniculitis-like T-cell lymphoma. Surprisingly, although 57% of patients had advanced stage disease and five patients relapsed after chemotherapy, the 5-year survival rate was 85.2%. However, treatment for PTCL was not consistent in this study. Eight patients received a regimen for T-cell lymphoma/leukemia, and four patients received a B cell lymphoma/leukemia regimen. Moreover, in one patient, symptoms improved spontaneously, and this has not previously been reported. Although five patients had relapse, four patients remained disease free at last follow-up and only two patients had undergone stem cell transplantation. Our study suggests that in the present population, PTCL in childhood does not have a poor outcome compared to adult with PTCL. This reason is not clear. However, the role of stem cell transplantation might be important. Stem cell transplantation had been undergone in eight patients with first complete response or partial response, one patient with progressive disease and two patients after relapse. After stem cell transplantation, only two patients died and nine patients are surviving without relapse.

Many cases of extranodal NK/T-cell lymphoma, nasal type were seen in this study compared with previous reports. Moreover, patients with this type of lymphoma were older at initial presentation than those with PTCL-NOS. Extranodal NK/T-cell lymphoma, nasal type is mostly confined to East Asia, and it predominantly occurs in the nasal or paranasal areas and less frequently in the skin. Most of the tumors show NK-cell phenotypes, although T-cell phenotypes are occasionally seen. The EB virus genome can usually be detected in lymphoma cells. Disease was associated with EB virus in 65% of patients with extranodal NK/T-cell lymphoma, nasal type compared with 50% of patients with PTCL-NOS. Suwiwat et al. [13] detected cell-free EBV DNA in 32/38 (84%) of adult PTCL patients, but failed to find EBV in controls. Rates of EB virus were higher in that report than in our study, possibly because Suwiwat et al. examined adults rather than children. However, we found EB virus in three of four patients who had HPS as the initial clinical feature. EB virus associated with HPS is sometimes seen in childhood, and some of these patients might also have PTCL. T-cell lymphoma-associated hemophagocytic syndrome (T-LAHS) has been frequently reported in Asian countries and is considered to have an extremely poor prognosis. Tong et al. [14] retrospectively analyzed the records of 113 patients with aggressive T-cell lymphoma, of which 28 had LAHS. The therapeutic results of chemotherapy alone or in combination with other modalities were discouraging for T-LAHS and the survival time for most patients was no more than 1 year. In the present study, unlike in other reports, three of four patients with HPS remained disease-free at last follow-up.

Pediatr Blood Cancer DOI 10.1002/pbc

TABLE I. Clinical Characteristics and Outcomes for 21 Patients With Peripheral T-Cell Lymphoma

	Age	Gender	Diagnosis	Initial lesion	Stage	Treatment	Response	Relapse	Transplantation	Association of EB virus	Survival time (months)
1	6	M	PTCL-NOS	Liver, spleen	4	JACLS NHL98ER	PR	N	Y	N	68+
2	4	F	PTCL-NOS	HPS	4	ALL (T)	CR	N	N	Y	60+
3	16	M	PTCL-NOS	Cervical	3	BFM NHL-T	PR	N	Y	N	36+
4	5	F	PTCL-NOS	Skin	1	JACLS NHL98T	CR	N	N	N	12+
5	7	M	PTCL-NOS	Cervical, HPS	1	None		N	N	Y	9+
6	9	M	PTCL-NOS	Cervical, spleen	3	TCCSG NHLT01	CR	N	N	ND	57+
7	11	F	PCTL-NOS	Cervical	1	T-LBL	CR	Y	Y	N	12
8	1	F	PTCL-NOS	HPS		VP16 + DEX	CR	N	Y	Y	30+
9	12	M	PTCL-NOS	Submandibular	3	CHOP	PR	N	Y	Y	30+
10	14	F	Subcutaneous panniculitis-like	Skin	2	Steroid	CR	N	Y	N	8+
11	14	M	AITL	Cervical	4	JACLS NHL98T	CR	N	N	N	96+
12	17	M	Extranodal NK/T nasal type	Adrenal grand, HPS	3	None		N	N	N	0
13	14	F	Extranodal NK/T nasal type	Skin	4	93mix	CR	N	Y	N	132+
14	21	F	Extranodal NK/T nasal type	Sinusoidal	4	HLH94	CR	Y	N	Y	30+
15	10	F	Extranodal NK/T nasal type	Orbit, breast	3	DeVIC	PD	Y	Y	N	36+
16	18	F	Extranodal NK/T nasal type	Nasal sinus, kidney, ovary	4	ALL (B)	PD	N	Y	Y	5
17	11	M	Extranodal NK/T nasal type	Skin	3	TCCSG NHL B96-04	CR	N	N	N	107+
18	18	M	Extranodal NK/T nasal type	Nasopharynx	2	Radiation	CR	Y	N	Y	105+
19	8	F	Extranodal NK/T nasal type	Skin	1	CCLSG NHL960LB	CR	N	N	Y	94+
20	10	M	Extranodal NK/T nasal type	Nasal sinus	1	DeVIC + radiation	CR	Y	Y	Y	45+
21	18	F	Extranodal NK/T nasal type	Nasal sinus, HPS	2	CHOP	PR	N	Y	Y	147+

PTCL-NOS, peripheral T-cell lymphoma, not otherwise specified; AITL, angioimmunoblastic T-cell lymphoma; HPS, hemophagocytic syndrome; CR, complete response, PR, partial response; PD, progressive disease; Y, yes; N, no; ND, no data. The drugs contained in remission introduction of each treatment is as follows: JACLS NHL98ER, vincristine (VCR), pirarubicin (THP-ADR), cyclophosphamide (CPM), L-asparaginase (L-asp), dexamethasone (DEX), prednisolone (PSL), JACLS NHL98T, VCR, CPM, adriamycin (ADR), L-asp, PSL, TCCSG NHLT01, VCR, CPM, ADR, L-asp, THPADR, PSL, CHOP: CPM, ADR, VCR, PSL, HLH94: etoposide (VP16), DEX, cyclosporine, DeVIC: DEX, ifosfamide, carboplatinum, VP16, TCCSG NHL B96-04: CPM, VP16, methotrexate (MTX), PSL, CCLSG NHL960LB: CPM, VCR, PRD, ADR, MTX.

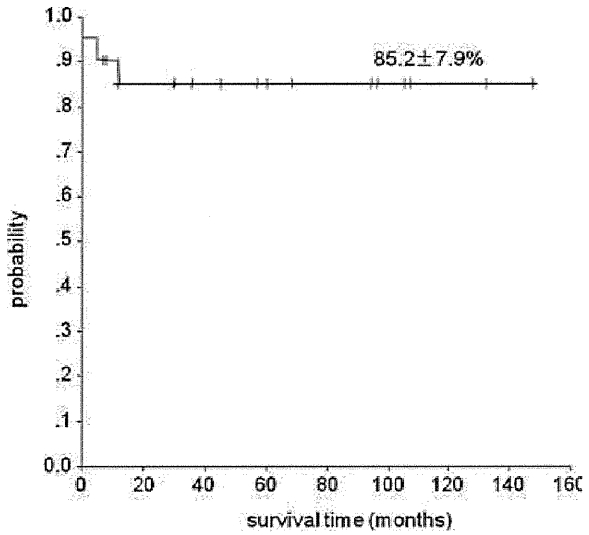

Fig. 1. Survival rate of patients with peripheral T-cell lymphoma. Five-year survival rate was 85.2%.

The findings of the present study differ from those of past reports of PTCL that included adults and children. However, the present study examined only a small number of patients. Larger studies are needed to confirm these findings.

ACKNOWLEDGMENT

This work was supported in part by a Grant for Clinical Cancer Research from the Ministry of Health, Labor and Welfare, Japan.

REFERENCES

1. International T-Cell Lymphoma Project. International peripheral T-cell and natural killer/T-cell lymphoma study: Pathology findings and clinical outcomes. J Clin Oncol 2008;26:4124–4130.
2. Savage KJ, Chhanabhai M, Gascoyne RD, et al. Characterization of peripheral T-cell lymphomas in a single North American institution by the WHO classification. Ann Oncol 2004;15:1467–1475.
3. Haioun C, Gaulard P, Bourquelot P, et al. Clinical and biological analysis of peripheral T-cell lymphomas: A single institution study. Leuk Lymphoma 1992;7:449–455.
4. Gisselbrecht C, Gaulard P, Lepage E, et al. Prognostic significance of T-cell phenotype in aggressive non-Hodgkin's lymphomas. Groupe d'Etudes des Lymphomes de l'Adulte (GELA). Blood 1998;92:76–82.
5. Arrowsmith ER, Macon WR, Kinney MC, et al. Peripheral T-cell lymphomas: Clinical features and prognostic factors of 92 cases defined by the Revised European American Lymphoma Classification. Leuk Lymphoma 2003;44:241–249.
6. Armitage JO, Vose JM, Linder J, et al. Clinical significance of the immunotype in diffuse aggressive non-Hodgkin's lymphoma. J Clin Oncol 1989;7:1783–1790.
7. Lim GY, Hahn ST, Chung NG, et al. Subcutaneous panniculitis-like T-cell lymphoma in a child: Whole-body MRI in the initial and follow-up evaluations. Pediatr Radiol 2009;39:57–61.
8. Windsor R, Stiller C, Webb D. Peripheral T-cell lymphoma in childhood: Population-based experience in the United Kingdom over 20 years. Pediatr Blood Cancer 2008;50:784–787.
9. Hutchison RE, Laver JH, Chang M, et al. Children's Oncology Group. Non-anaplastic peripheral t-cell lymphoma in childhood and adolescence: A Children's Oncology Group study. Pediatr Blood Cancer 2008;51:29–33.
10. Brodkin DE, Hobohm DW, Nigam R. Nasal-type NK/T-cell lymphoma presenting as hemophagocytic syndrome in an 11-year-old Mexican boy. J Pediatr Hematol Oncol 2008;30: 938–940.
11. Medhi K, Kumar R, Rishi A, et al. Subcutaneous panniculitislike T-cell lymphoma with hemophagocytosis: Complete remission with BFM-90 protocol. J Pediatr Hematol Oncol 2008;30:558–561.
12. Tsai ST, Jin YT, Wu TC. Synthesis of PCR-derived, digoxigenin-labeled DNA probes for in situ detection of Epstein-Barr early RNAs in Epstein-Barr virus-infected cells. J Virol Methods 1995; 54:67–74.
13. Suwiwat S, Pradutkanchana J, Ishida T, et al. Quantitative analysis of cell-free Epstein-Barr virus DNA in the plasma of patients with peripheral T-cell and NK-cell lymphomas and peripheral T-cell proliferative diseases. J Clin Virol 2007;40:277–283.
14. Tong H, Ren Y, Liu H, et al. Clinical characteristics of T-cell lymphoma associated with hemophagocytic syndrome: Comparison of T-cell lymphoma with and without hemophagocytic syndrome. Leuk Lymphoma 2008;49:81–87.

Leukemia (2010) 24, 335–344

www.nature.com/leu

EDUCATIONAL REPORT

Long-term results of the Japanese Childhood Cancer and Leukemia Study Group studies 811, 841, 874 and 911 on childhood acute lymphoblastic leukemia

M Tsurusawa[1], Y Shimomura[1], K Asami[2], A Kikuta[3], A Watanabe[4], Y Horikoshi[5], T Matsushita[6], H Kanegane[7], S Ohta[8], A Iwai[9], H Mugishima[10] and S Koizumi[11] for the Japanese Childhood Cancer and Leukemia Study Group

[1]Department of Pediatrics, Aichi Medical University, Aichi, Japan; [2]Department of Pediatrics, Niigata Cancer Center Hospital, Niigata, Japan; [3]Department of Pediatrics, Fukushima Medical School, Fukushima, Japan; [4]Department of Pediatrics, Nakadori Hospital, Akita, Japan; [5]Division of Hematology and Oncology, Shizuoka Children's Hospital, Shizuoka, Japan; [6]Department of Pediatrics, International Medical Center of Japan, Tokyo, Japan; [7]Department of Pediatrics, Toyama Medical and Pharmaceutical University, Toyama, Japan; [8]Department of Pediatrics, Shiga Medical School, Shiga, Japan; [9]Division of Pediatrics, Kagawa National Children's Hospital, Kagawa, Japan; [10]Department of Pediatrics, Nihon University, Itabashi Hospital, Tokyo, Japan and [11]Department of Pediatrics, Graduate School of Medical Science, Kanazawa University, Ishikawa, Japan

We analyzed the long-term outcomes of 1021 patients with acute lymphoblastic leukemia (ALL), enrolled in four successive clinical trials (ALL811, ALL841, ALL874 and ALL911) between 1981 and 1993. All patients received risk-adopted therapy according to leukocyte count and age at the time of diagnosis. The median follow-up durations of the four studies were 17.8 years in ALL811, 15.5 years in ALL841, 11.9 years in ALL874 and 15.8 years in ALL911. Patients' event-free survival (EFS) and overall survival (OS) rates at 12 years were 41.0 and 54.3% in ALL811, 50.2 and 60.2% in ALL841, 57.3 and 64.7% in ALL874, and 63.4 and 71.7% in ALL911, respectively. Thus, cure can become a reality for about 70% of children with ALL. There is, however, still a significant difference in survival outcomes according to risk group. Late effects were observed in 70 patients out of 834 (8.4%); hepatitis and short stature were most commonly reported. Reduction of late adverse effects for all patients and development of new treatment strategies for very-high-risk patients are major issues for upcoming trials to address.
Leukemia (2010) **24,** 335–344; doi:10.1038/leu.2009.259; published online 17 December 2009
Keywords: childhood; acute lymphoblastic leukemia; long-term outcome

Introduction

The therapeutic experience of acute lymphoblastic leukemia (ALL) is one of the true success stories of modern clinical oncology. Incremental advances in treatment success span a 50-year period during which ALL has progressed from a uniformly fatal disease to an illness with an overall cure rate of 75–85%.[1–4] This extraordinary progress has resulted from advances in treatment beginning with the identification of effective single-agent chemotherapy in the late 1940s, followed by development of combination and maintenance chemotherapy and introduction of central nervous system (CNS) preventive therapy in the 1960s. Tailoring therapy according to risk factors, followed by more intensified chemotherapy with improvements in supportive care, further increased the cure rate from the 1980s through early 1990s. On the other hand, late adverse effects have become an important issue disturbing the quality of life of long-term survivors.

Correspondence: Professor M Tsurusawa, Department of Pediatrics, Aichi Medical University, Nagakute-cho, Aichi-gun, Aichi 480-1195, Japan.
E-mail: mtsuru@aichi-med-u.ac.jp
Received 17 October 2009; accepted 23 October 2009; published online 17 December 2009

For over 25 years, we have conducted successive clinical trials (ALL811, ALL841, ALL874, ALL911, ALL941 and ALL2000) on children with ALL, and have achieved consistent improvement in treatment outcomes.[5–12] Here, we show long-term outcomes of patients treated from the early 1980s through the mid 1990s (ALL811, ALL841, ALL874 and ALL911), and also discuss late adverse effects.

Materials and methods

Patients

A total of 1021 untreated ALL patients below 18 years of age were registered to participate in a series of Japanese Childhood Cancer and Leukemia Study Group (JCCLSG) trials (ALL811, ALL841, ALL874 and ALL911) conducted in 21 hospitals, all of which were members of the JCCLSG. Written informed consent was provided by patients or legal guardians before treatment. ALL diagnoses were based on cytomorphology (FAB criteria, L1/L2) and cytochemistry when ≧25% lymphoblastic cells were present in bone marrow samples. Flow-cytometric immunophenotyping was performed only for patients in the ALL911 studies at the central laboratory (Aichi Medical University), but was not mandatory. Based on age and leukocyte count at diagnosis,[6] patients were stratified into one of the following groups: low-risk (LR), intermediate-risk (IR) or high-risk (HR). In ALL811, patients in the LR or IR group were defined as the standard-risk (SR) group.[7] Of HR patients in ALL911, cases with initial leukocyte count greater than 100×10^9/l were further stratified into a 'high-high-risk' (HHR) group (Table 1).

Treatment protocols

Details of treatment protocols have been described in earlier publications.[7–10] An outline of treatment regimens in the protocols and detailed therapy schedules, including drug dosage, are provided in Tables 2 and 3, respectively.

ALL811. The main aim of the S811 protocol was a randomized control study of two different maintenance chemotherapies.[7] SR patients received a two-drug (VP) induction therapy consisting of vincristine (VCR) and prednisolone (PSL). After achieving complete remission, they were randomized to either arm-A, consisting of intermittent cyclic administration of four drugs (VPM-M regimen), VCR, PSL, 6-mercaptopurine (6MP) and intermediate-dose methotrexate (MTX), or arm-B, consisting of

continuous low-dose MTX and 6MP combined with VP pulse. HR patients were randomly assigned to the H811A or H811B arms to compare the high-dose (HD) MTX and cranial irradiation (CRT) regimens for CNS prophylaxis. In the H811A arm, doxorubicin (DOX) was employed as consolidation therapy.

ALL841. The main aim of this study was improvement of induction therapy. Patients in the LR group were assigned randomly to the two-drug induction regimen (VP) in the L841A arm or a three-drug regimen (VP plus L-asparaginase,LASP) in the L841B arm. The maintenance therapy consisted of the VPM-ML regimen in L841A or the VPM-ML regimen incorporating LASP in L841B. In HR patients, the efficacy of addition of cyclophosphamide (CPM) in induction and maintenance therapy was studied in the H851A and H851B arms. Starting in 1985, the treatment lasted 3 years after the point of achieving complete remission for all patients.

Table 1 Risk classification of ALL according to age and leukocyte count at diagnosis

WBC count $\times 10^9$/l	*Age (years)*[a]			
	1–3	*4–5*	*6–9*	*≧10*
≦5	LR (SR)	LR (SR)	IR (SR)	HR
>5, ≦10	LR (SR)	IR (SR)	HR	HR
>10, ≦50	IR (SR)	IR (SR)	HR	HR
>50	HR	HR	HR	HR
(>100)	(HHR)	(HHR)	(HHR)	(HHR)

Abbreviations: ALL, acute lymphoblastic leukemia; HR, high risk; HHR, high-high risk; IR, intermediate risk; LR, low risk; SR, standard risk.
[a]Patients < 1 year were assigned into IR (WBC count $\leqslant 10 \times 10^9$/l) or HR (WBC count $>10 \times 10^9$/l) group.

ALL874. The primary aim of this study was to clarify whether CNS-protective chemotherapy without CRT for treatment of non-HR patients could be accepted without compromising outcomes delivered by conventional CRT regimens. LR and IR patients were assigned randomly to the conventional CRT regimen (L874A and I874A) and the HDMTX regimen without CRT (L874B and I874B). In the HR group, the consolidation regimen of intermediate-dose CPM and cytarabine (Ara-C) (CCM regimen) was compared with the regimen of high-dose CPM and Ara-C (CC regimen). In addition, reinduction therapy (VPLA) was newly employed at months 5 and 12 of therapy. The duration of treatment was 3 years for all patients, as in the ALL841 study.

ALL911. The primary aim of this study was to improve HR patient outcomes. For this, we further stratified HR patients into two groups of HR and HHR, with the latter group receiving more intensified chemotherapy. For this study, a non-randomized, single-arm study was selected because of the small number of patients per subset. The four-drug regimen (VPLA/VPLA′) was used as an induction therapy for all patients, and a tetrahydropyranyl derivative of DOX (pirarubicin, THP) was used instead of DOX as the VPLA′ regimen for LR and IR patients. The IR, HR and HHR groups received the same consolidation (CCM) and reinduction therapy (VLPA′). For CNS prophylaxis, CRT was omitted for the LR and IR patients. The duration of treatment was 2 years for the LR group and 3 years for the other three groups.

Late effects

A set of written questions on late adverse effects on patients treated with one of the four protocols (ALL811, ALL841, ALL874 and ALL911) was sent to all participating institutes in

Table 2 Outlines of JCCLSG protocols for childhood ALL

Study	*Protocols*	*Remission induction*	*Consolidation*	*Reinduction*	*CNS prophylaxis*[a]	*Maintenance chemotherapy*
ALL811	S811A	VP	—	—	CRT (18 Gy)	VPM-M
	S811B	As in S811A	—	—	As in S811A	MM-VP
	H811A	VPC	DOX ×3	—	HDMTX	VPM-HDMTX
	H811B	VPCA	—	—	CRT (18 Gy)	VPM-M-AC
ALL841	L841A	VP	—	—	CRT (18 Gy)	VPM-M
	L841B	VPL	—	—	As in L841A	VPM-ML
	I841B	As in L841B	—	—	As in L841A	As in L841B
	I841C	As in L841B	DOX ×4	—	HDMTX	VPM-M-AC
	H851A	VPC	As in I841C	—	HDMTX	VPM-HDMTX
	H851B	As in H851A	As in I841C	—	As in H851A	As in I841C
ALL874	L874A	VPL		—	CRT (18 Gy)	VPM-M
	L874B	As in L874A	—	—	HDMTX	As in L874A
	I874A	As in L874A	—	—	CRT (18 Gy)	VPMA-HDMTX
	I874B	As in L874A	—	—	HDMTX	As in I874A
	H874A	VPLA	CCM ×3	VPLA	CRT (24 Gy)+HDMTX	As in L874A
	H874B	As in 874A	CC ×3	As in 874A	As in H874A	As in L874A
ALL911	L911	VPLA′	—	—	HDMTX	VPMA-M
	I911	As in L911	CCM ×2	VPLA′	TIT	VPMA-M/VPM-M[b]
	H911	VPLA	CCM ×3	VPLA′ ×2	CRT (18 Gy)	As in I911
	HH911	As in H911	As in H911	As in H911	CRT (24 Gy)	VPMA-M-EC/VPM-M-EC[b]

Abbreviations: ALL, acute lymphoblastic leukemia; CRT, cranial irradiation; DOX, doxorubicin; HDMTX, high-dose methotrexate; JCCLSG, Japanese Childhood Cancer and Leukemia Study Group; TIT, triple intrathecal therapy; VP, vincristine+prednisolone; VPC, vincristine+prednisolone+cyclophosphamide; VPCA, vincristine+prednisolone+cyclophosphamide+doxorubicin; VPL, vincristine+prednisolone+L-asparaginase; VPLA, VPL+doxorubicin; VPLA′, VPL+pirarubicin.
[a]Proportion of patients who received prophylactic CRT in each study: 138/207 (66.6%) in ALL811, 85/220 (38.6%) in ALL841, 275/371 (74.1%) in ALL874 and 110/223 (49.3%) in ALL911.
[b]Anthracycline (DOX/THP) was omitted in the second and third years.

Table 3 Drug dosage and schedules for the JCCLSG ALL protocols

Regimen		*Administration*	*Daily dose*	*Days*
Induction phase				
VP	Vincristine	IV	2 mg/m^2	1, 8, 15, 22
	Prednisolone	Orally	60 mg/m^2	1–28
VPC (VP+CPM)	Cyclophosphamide	IV	1.2 g/m^2	1
VPCA (VP+CPM+DOX)	Cyclophosphamide	IV	300 mg/m^2	15
	Doxorubicin	IV	20 mg/m^2	1
VPL (VP+LASP)	L-asparaginase	IV	2000 U/m^2	1, 3, 5, 8, 10, 12, 15, 17, 19
VPLA (VPL+DOX)	Doxorubicin	IV	25 mg/m^2	8, 15, 22
VPLA′ (VPL+THP)	Pirarubicin	IV	30 mg/m^2	8, 15, 22
Consolidation phase				
DOX	Doxorubicin	IV	20 mg/m^2	1–4
CCM	Cyclophosphamide	IV	400 mg/m^2	1, 15
	Cytarabine	IV	75 mg/m^2 ×2	1–4, 15–18
	6-Mercaptopurine	Orally	60 mg/m^2	1–28
CC	Cyclophosphamide	IV	1.2 g/m^2	1
	Cytarabine	IV	1.5 g/m^2 ×2	15, 16
EC	Etoposide	IV	100 mg/m^2	1–3
	Cytarabine	IV	2 g/m^2 ×2	1–4
CNS prophylaxis				
See Table 6				
Maintenance phase				
VPM-M	Vincristine	IV	2 mg/m^2	1
	Prednisolone	Orally	120 mg/m^2	1–5
	6-Mercaptopurine	Orally	175 mg/m^2	1–5
	Methotrexate	IV	225 mg/m^2	14
MM-VP	6-Mercaptopurine	Orally	50 mg/m^2	1–28
	Methotrexate	Orally	20 mg/m^2	1–28
	Vincristine	IV	2 mg/m^2	1
	Prednisolone	Orally	120 mg/m^2	1–5
VPM-ML	Similar to VPM-M except for 6MP (250 mg/m^2) and LASP (2000 U/m^2), every 4 weeks			
VPM-M-AC	Similar to VPM-M except for CPM (300 mg/m^2), day 28 & DOX (20 mg/m^2), day 1			
VPM-HDMTX	Similar to VPM-M except for HDMTX (6 g/m^2), every 4 weeks			
VPMA-HDMTX	Similar to VPMA-M except for HDMTX (4.5 g/m^2), every 6 weeks.			
VPMA-M	Similar to VPM-M except for DOX 20 mg/m^2 or THP 30 mg/m^2, day 1			
VPMA-M-EC	Similar to VPMA-M except for VP16 (150 mg/m^2) and Ara-C (300 mg/m^2), day 28			
VPM-M-EC	Similar to VPM-M except for VP16 (150 mg/m^2) and Ara-C (300 mg/m^2), day 28			

Abbreviations: ALL, acute lymphoblastic leukemia; Ara-C, cytarabine; HDMTX, high-dose methotrexate; IV, intravenous; JCCLSG, Japanese Childhood Cancer and Leukemia Study Group.

March 2002, and the questionnaire was collected in June that year.

Statistical analysis

Final statistical analyses of ALL911 patients were based on data obtained in June 2008, while those of subjects in the ALL811, ALL841 and ALL874 studies used data obtained in June 2001, when the final survey on outcomes was taken. Survival curves were prepared by the Kaplan–Meier method and a log-rank test was used to detect significant differences between groups. Overall survival (OS) was defined as the time between disease diagnosis and death, and event-free survival (EFS) was defined as the time to first occurrence of induction failure, relapse at any site, death or secondary malignant neoplasm. For patients who experienced no events, EFS was the time to the most recent follow-up. CNS relapse-free survival and bone marrow relapse-free survival were measured from the end of induction and excluded patients who failed to achieve complete remission. The SPSS statistical analysis software (SPSS 12.0J, Japan Inc., Tokyo, Japan) was used for all computations.

Results

Survival outcomes

Long-term survival curves for patients over the four ALL studies are presented in Figure 1. The median follow-up duration of the four studies was as follows: 17.8 years (range 3.1–20.5 years) for 110 survivors in ALL811, 15.5 years (5.1–17.3 years) for 131 survivors in ALL841, 11.9 years (5.3–14.1 years) for 235 survivors in ALL874 and 15.8 years (4.3–18.3 years) for 159 survivors in ALL911. Their EFS and OS at 12 years were 41.0 ± 3.6 and 54.3 ± 3.3% in ALL811 (n = 207), 50.2 ± 3.5 and 60.2 ± 3.3% in ALL841 (n = 220), 57.3 ± 2.7 and 64.7 ± 2.5% in ALL874 (n = 371), and 63.4 ± 3.3 and 71.7 ± 3.0% in ALL911 (n = 223).

Treatment outcomes

Treatment outcomes for the four ALL studies are shown in Table 4 and survival outcomes at 5-year intervals according to treatment protocol and presenting features are shown in Tables 5a–5d.

ALL811. A total of 230 children were enrolled in the ALL811 study, of which 207 patients were evaluable. Ages ranged from